

A class of refined implicit-explicit Runge-Kutta methods with robust time adaptability and unconditional convergence for the Cahn-Hilliard model

Hong-lin Liao* Tao Tang[†] Xuping Wang[‡] Tao Zhou[§]

December 11, 2024

Abstract

One of main obstacles in verifying the energy dissipation laws of implicit-explicit Runge-Kutta (IERK) methods for phase field equations is to establish the uniform boundedness of stage solutions without the global Lipschitz continuity assumption of nonlinear bulk. With the help of discrete orthogonal convolution kernels, an updated time-space splitting technique is developed to establish the uniform boundedness of stage solutions for a refined class of IERK methods in which the associated differentiation matrices and the average dissipation rates are always independent of the time-space discretization meshes. This makes the refined IERK methods highly advantageous in self-adaptive time-stepping procedures as some larger adaptive step-sizes in actual simulations become possible. From the perspective of optimizing the average dissipation rate, we construct some parameterized refined IERK methods up to third-order accuracy, in which the involved diagonally implicit Runge-Kutta methods for the implicit part have an explicit first stage and allow a stage-order of two such that they are not necessarily algebraically stable. Then we are able to establish, for the first time, the original energy dissipation law and the unconditional L^2 norm convergence. Extensive numerical tests are presented to support our theory.

KEYWORDS: Cahn-Hilliard model, implicit-explicit Runge-Kutta method, average dissipation rate, robust time adaptability, unconditional L^2 norm, original energy dissipation law

AMS subject classifications: 35K58, 65L20, 65M06, 65M12

1 Introduction

The aim of this work is to present a class of refined implicit-explicit Runge-Kutta methods with robust time adaptability and unconditional convergence for the Cahn-Hilliard model. In our previous work [26], a unified theoretical framework was suggested to examine the energy dissipation properties

*ORCID 0000-0003-0777-6832. School of Mathematics, Nanjing University of Aeronautics and Astronautics, Nanjing 211106, China; Key Laboratory of Mathematical Modeling and High Performance Computing of Air Vehicles (NUAA), MIIT, Nanjing 211106, China. Emails: liaohl@nuaa.edu.cn and liaohl@csrc.ac.cn. This author is supported by NSF of China under grant numbers 12471383 and 12071216.

[†]School of Electrical and Computer Engineering, Guangzhou Nanfang College, and Institute for Advanced Study, BNU-HKBU United International College, China. Email: ttang@uic.edu.cn. This author is supported by NSF of China under grant numbers 11731006 and K20911001.

[‡]School of Mathematics, Nanjing University of Aeronautics and Astronautics, Nanjing 211106, China. Email: wangxp@nuaa.edu.cn.

[§]Institute of Computational Mathematics and Scientific/Engineering Computing, Academy of Mathematics and Systems Science, Chinese Academy of Sciences, Beijing, 100190, China. Email: tzhou@lsec.cc.ac.cn. This author is supported by NSF of China under grant number 12288201.

at all stages of additive implicit-explicit Runge-Kutta (IERK) methods up to fourth-order accuracy for gradient flow problems. Some parameterized IERK methods preserving the original energy dissipation law unconditionally were constructed by applying the so-called first same as last method, that is, the diagonally implicit Runge-Kutta (DIRK) method with the explicit first stage and stiffly-accurate assumption for the linear stiff term, and applying the explicit Runge-Kutta method for the nonlinear term. The main idea in [26] is to construct the differential forms and the associated differentiation matrices of IERK methods by using the difference coefficients of method and the so-called discrete orthogonal convolution kernels [22, 23, 27]. Nonetheless, this theory was built on a strong assumption: the involved nonlinear terms are globally Lipschitz continuous.

In this work, we will consider a much more practical assumption: the nonlinear term is continuously differentiable. Under this assumption, we shall perform a unified L^2 norm convergence analysis of a refined class of IERK methods and establish the associated original energy dissipation laws for the well-known Cahn-Hilliard (CH) equation. To the best of our knowledge, this is the first time such original energy dissipation law and unconditional L^2 norm convergence of IERK methods are established for the CH model without the global Lipschitz continuity assumption of the nonlinear bulk.

Consider a free energy functional of Ginzburg-Landau type,

$$E[\Phi] = \int_{\Omega} \left[\frac{\epsilon^2}{2} |\nabla \Phi|^2 + F(\Phi) \right] d\mathbf{x} \quad \text{with} \quad F(\Phi) := \frac{1}{4} (\Phi^2 - 1)^2, \quad (1.1)$$

where $\mathbf{x} \in \Omega \subseteq \mathbb{R}^2$ and $0 < \epsilon < 1$ is proportional to the interface width. The well known Cahn-Hilliard equation is given by the H^{-1} gradient flow associated with the free energy functional $E[\Phi]$,

$$\partial_t \Phi = \Delta [F'(\Phi) - \epsilon^2 \Delta \Phi] \quad \text{for } \mathbf{x} \in \Omega. \quad (1.2)$$

Assume that Φ is periodic over the domain Ω . By applying the integration by parts, one can find the volume conservation, $(\Phi(t), 1) = (\Phi(t_0), 1)$, and the following original energy dissipation law,

$$\frac{dE}{dt} = \left(\frac{\delta E}{\delta \Phi}, \partial_t \Phi \right)_{L^2} = - \left((-\Delta)^{-1} \partial_t \Phi, \partial_t \Phi \right)_{L^2} \leq 0, \quad (1.3)$$

where the L^2 inner product $(u, v)_{L^2} := \int_{\Omega} uv \, d\mathbf{x}$ for all $u, v \in L^2(\Omega)$.

Always, the explicit approximation of the nonlinear bulk f will be adopted in our IERK methods so that they are computationally efficient by avoiding the inner iteration at each time stage. To control the possible instability stemmed from the explicit approximation of f , we introduce the following stabilized operators with the stabilized parameter $\kappa \geq 0$, cf. [7, 8, 24, 25],

$$L_{\kappa} \Phi := -\epsilon^2 \Delta \Phi + \kappa \Phi \quad \text{and} \quad f_{\kappa}(\Phi) := \kappa \Phi - F'(\Phi), \quad (1.4)$$

such that the problem (1.2) becomes the stabilized version

$$\partial_t \Phi = \Delta [L_{\kappa} \Phi - f_{\kappa}(\Phi)] \quad \text{for } \mathbf{x} \in \Omega. \quad (1.5)$$

Interested readers are referred to the series [14–17], where Li et al. characterized the sizes of stabilization parameter for a wide class of semi-implicit stabilized methods for the CH model.

We apply the Fourier pseudo-spectral method to approximate the spatial operators Δ and L_{κ} , as described in Section 2, with the associated discrete operators (matrices) Δ_h and $L_{\kappa, h}$, respectively. For a finite T , consider a nonuniform mesh $0 = t_0 < t_1 < \dots < t_N = T$ with the time-step $\tau_n = t_n - t_{n-1}$. The time operator is approximated by IERK methods and let ϕ_h^k be the numerical approximation of $\Phi_h^k := \Phi(\mathbf{x}_h, t_k)$ at the discrete time level t_k for $0 \leq k \leq N$. For a s -stage Runge-Kutta method, let $u_h^{n, i}$ be the approximation of $\Phi_h^{n, i} := \Phi(\mathbf{x}_h, t_{n-1} + c_i \tau_n)$ at the abscissas $c_1 := 0$, $c_i > 0$ for $2 \leq i \leq s-1$,

and $c_s := 1$. To integrate the nonlinear model (1.5) from t_{n-1} ($n \geq 1$) to the next grid point t_n , we consider the following s -stage IERK method [2, 8, 26, 31, 32]

$$u_h^{n,i} := u_h^{n,1} + \tau_n \sum_{j=1}^i a_{i,j} \Delta_h L_{\kappa,h} u_h^{n,j} - \tau_n \sum_{j=1}^{i-1} \hat{a}_{i,j} \Delta_h f_{\kappa}(u_h^{n,j}) \quad \text{for } n \geq 1 \text{ and } 1 \leq i \leq s, \quad (1.6)$$

where $u_h^{n,1} := \phi_h^{n-1}$ and $\phi_h^n := u_h^{n,s}$. The associated Butcher tableaux reads

$$\begin{array}{c|ccc} \mathbf{c} & A & & \\ \mathbf{b}^T & & & \end{array} = \begin{array}{c|ccc} c_1 & 0 & & \\ c_2 & a_{21} & a_{22} & \\ c_3 & a_{31} & a_{32} & a_{33} \\ \vdots & \vdots & \vdots & \ddots & \ddots \\ c_s & a_{s,1} & a_{s,2} & \cdots & a_{s,s-1} & a_{s,s} \\ \hline & a_{s,1} & a_{s,2} & \cdots & a_{s,s-1} & a_{s,s} \end{array}, \quad \begin{array}{c|ccc} \mathbf{c} & \hat{A} & & \\ \hat{\mathbf{b}}^T & & & \end{array} = \begin{array}{c|ccc} c_1 & 0 & & \\ c_2 & \hat{a}_{21} & 0 & \\ c_3 & \hat{a}_{31} & \hat{a}_{32} & 0 \\ \vdots & \vdots & \vdots & \ddots & \ddots \\ c_s & \hat{a}_{s,1} & \hat{a}_{s,2} & \cdots & \hat{a}_{s,s-1} & 0 \\ \hline & \hat{a}_{s,1} & \hat{a}_{s,2} & \cdots & \hat{a}_{s,s-1} & 0 \end{array}$$

Without losing the generality, we always assume that $\hat{a}_{k+1,k}(z) \neq 0$ for any $1 \leq k \leq s-1$. That is, the stiff linear term L_{κ} is approximated by the s -stage stiffly-accurate DIRK method with the coefficient matrix A , the abscissa vector $\mathbf{c} = A\mathbf{1}$ and the vector of weights $\mathbf{b} := A^T \mathbf{e}_s$, while the nonlinear term f_{κ} is approximated by the s -stage explicit Runge-Kutta methods with the strictly lower triangular coefficient matrix \hat{A} , the abscissa vector $\hat{\mathbf{c}} = \hat{A}\mathbf{1}$ and the vector of weights $\hat{\mathbf{b}} := \hat{A}^T \mathbf{e}_s$. Here we impose the canopy node condition, $\hat{\mathbf{c}} = \mathbf{c}$ or $A\mathbf{1} = \hat{A}\mathbf{1}$, such that the IERK method (1.6) is consistent at all stages. Table 1 lists the order conditions for the coefficients matrices and the weight vectors to make the IERK method (1.6) to be accurate up to third-order in time. A detailed description of these order conditions can also be found in [2, 11, 32].

Table 1: Order conditions for IERK methods up to third-order.

Order	Stand-alone conditions		Coupling condition
	Implicit part	Explicit part	
1	$\mathbf{b}^T \mathbf{1} = 1$	$\hat{\mathbf{b}}^T \mathbf{1} = 1$	-
2	$\mathbf{b}^T \mathbf{c} = \frac{1}{2}$	$\hat{\mathbf{b}}^T \mathbf{c} = \frac{1}{2}$	-
3	$\mathbf{b}^T \mathbf{c}^2 = \frac{1}{3}$ $\mathbf{b}^T A \mathbf{c} = \frac{1}{6}$	$\hat{\mathbf{b}}^T \mathbf{c}^2 = \frac{1}{3}$ $\hat{\mathbf{b}}^T \hat{A} \mathbf{c} = \frac{1}{6}$	$\mathbf{b}^T \hat{A} \mathbf{c} = \frac{1}{6}, \hat{\mathbf{b}}^T A \mathbf{c} = \frac{1}{6}$

* For the vectors \mathbf{x} and \mathbf{y} , $\mathbf{x} \odot \mathbf{y} := (x_1 y_1, x_2 y_2, \dots, x_s y_s)^T$ and $\mathbf{x}^m := \mathbf{x} \odot \mathbf{x}^{(m-1)}$ for $m > 1$.

Moreover, requiring $u_h^{n,i} = \phi_h^*$ for all i and $n \geq 1$ immediately shows that the canopy node condition $\hat{\mathbf{c}} = \mathbf{c}$ makes the IERK method (1.6) preserve naturally the equilibria ϕ^* of the CH model (1.5), that is, $\epsilon^2 \Delta_h \phi_h^* = F'(\phi_h^*)$ or $L_{\kappa,h} \phi_h^* = f_{\kappa}(\phi_h^*)$. So one can reformulate the standard form (1.6) into the following steady-state preserving form

$$\begin{aligned} u_h^{n,i+1} &= u_h^{n,1} + \tau_n \sum_{j=1}^{i+1} a_{i+1,j} \Delta_h (L_{\kappa,h} u_h^{n,j} - L_{\kappa,h} u_h^{n,1}) - \tau_n \sum_{j=1}^i \hat{a}_{i+1,j} \Delta_h [f_{\kappa}(u_h^{n,j}) - L_{\kappa,h} u_h^{n,1}] \\ &= u_h^{n,1} + \tau_n \sum_{j=1}^i a_{i+1,j+1} \Delta_h (L_{\kappa,h} u_h^{n,j+1} - L_{\kappa,h} u_h^{n,1}) - \tau_n \sum_{j=1}^i \hat{a}_{i+1,j} \Delta_h [f_{\kappa}(u_h^{n,j}) - L_{\kappa,h} u_h^{n,1}] \end{aligned} \quad (1.7)$$

for $1 \leq i \leq s_I := s - 1$ (s_I represents the number of implicit stages), in which we drop the terms with the coefficients $a_{i+1,1}$ for $1 \leq i \leq s_I$. In this sense, we define the lower triangular coefficient matrices for the implicit and explicit parts, respectively,

$$A_I := (a_{i+1,j+1})_{i,j=1}^{s_I} \quad \text{and} \quad A_E := (\hat{a}_{i+1,j})_{i,j=1}^{s_I}.$$

Note that, the two matrices A_I and A_E are always required in our theory, while the coefficient vector $\mathbf{a}_1 := (a_{21}, a_{31}, \dots, a_{s1})^T$ would be not involved directly although it would be useful in designing some computationally effective IERK methods. If $\mathbf{a}_1 \neq \mathbf{0}$, the Lobatto-type DIRK methods are used in the implicit part and the associated method (1.6) is called Lobatto-type IERK methods; while we call (1.6) as Radau-type (known as ARS-type [2]) IERK methods if $\mathbf{a}_1 = \mathbf{0}$.

Actually, to avoid nonlinear iteration at each stage of implicit Runge-Kutta methods, the IERK methods have attracted much attention [2, 3, 8, 11, 12, 26, 31, 32]. Kennedy and Carpenter [12] constructed high-order IERK methods from third- to fifth-order to simulate convection-diffusion-reaction equations. The widespread ARS-type IERK methods were developed in [2] to solve the convection-diffusion problems. Cardone et al. [3] proposed a class of ARS-type IERK methods up to fourth-order based on the extrapolation of stage solutions at the current and previous steps. Izzo and Jackiewicz [11] constructed some parameterized IERK methods up to fourth-order with A-stable implicit part by choosing the method parameters to maximize the regions of absolute stability for the explicit part. In simulating the semilinear parabolic problems, IERK methods turned out to be very competitive. Shin et al. [31] observed that the Radau-type IERK methods combined with convex splitting technique exhibit the original energy stability in numerical experiments, and established the energy stability in [32] for a special case. Recently, Fu et al. [8] derived some sufficient conditions of Radau-type IERK methods to maintain the decay of original energy for the gradient flow problems with the global Lipschitz continuity assumption of nonlinear bulk, and presented some concrete schemes up to third-order accuracy. However, the rigorous stability and convergence of these (not algebraically stable) IERK methods for the CH model (1.2) are rather difficult because it is technically challenging to verify the uniform boundedness of stage solutions for multi-stage methods [8, 31, 32].

In the literature, there are many works on linearized time-stepping methods and the numerical analysis for the CH model (1.2). Sun [34] developed three-level Crank-Nicolson type method with finite difference approximation in space, and Li et al. [20] established the unconditional convergence of the three-level linearized time-stepping method in the maximum norm. Second-order energy-stable semi-implicit approaches were constructed and analyzed in [9, 35]. In resolving the long-time multi-scale dynamics, variable-step time-stepping approaches were developed and analyzed in [4, 23, 36], in which the robust stability and convergence with respect to the change of time-step sizes are established. Combining the scalar auxiliary variable method [30] and the Gaussian Runge-Kutta methods, arbitrarily high-order energy-stable schemes were constructed in [1], while the energy stability was established with respect to a modified energy involving the auxiliary variable. Related works on energy stable time-stepping methods can be also found in [6, 8, 10, 28, 30] and the reference therein, with certain modified discrete energy functional by adding some nonnegative small terms to the original energy (1.1), especially for high-order multi-step approaches.

In the next section, we present the theoretical and numerical motivations to a refined class of Lobatto-type IERK methods, called refined IERK (R-IERK), in which the associated differentiation matrices and the average dissipation rates are independent of the time-space discretization meshes. Some parameterized R-IERK methods up to third-order accuracy are constructed in Section 3. The unconditional L^2 norm error estimate and the original energy dissipation law of R-IERK methods are addressed in Section 4 with an updated technique of time-space error splitting. Extensive experiments are presented in Section 5 to support our theory and show the effectiveness of R-IERK methods.

For simplicity, we will use the simplified notations, IERK($p, s; \mu$) and R-IERK($p, s; \mu$), to represent the p -th order s -stage μ -parameterized IERK and R-IERK methods, respectively. Always, we use $D_{\mathbb{R}}^{(p,s)}$ and $\mathcal{R}_{\mathbb{R}}^{(p,s)}$ to represent the associated differentiation matrix and the average dissipation rate, respectively, of a p -th order s -stage R-IERK method.

2 Theoretical and numerical motivations

Set the domain $\Omega = (0, L)^2$ and consider the uniform length $h_x = h_y = h := L/M$ in each direction for an even positive integer M . Let $\Omega_h := \{\mathbf{x}_h = (ih, jh) \mid 1 \leq i, j \leq M\}$ and put $\bar{\Omega}_h := \Omega_h \cup \partial\Omega$. Denote the space of L -periodic grid functions $\mathbb{V}_h := \{v \mid v = (v_h) \text{ is } L\text{-periodic for } \mathbf{x}_h \in \bar{\Omega}_h\}$. For a periodic function $v(\mathbf{x})$ on $\bar{\Omega}$, let $P_M : L^2(\Omega) \rightarrow \mathcal{F}_M$ be the standard L^2 projection operator onto the space \mathcal{F}_M , consisting of all trigonometric polynomials of degree up to $M/2$, and $I_M : L^2(\Omega) \rightarrow \mathcal{F}_M$ be the trigonometric interpolation operator [29], i.e.,

$$(P_M v)(\mathbf{x}) = \sum_{\ell, m=-M/2}^{M/2-1} \widehat{v}_{\ell, m} e_{\ell, m}(\mathbf{x}), \quad (I_M v)(\mathbf{x}) = \sum_{\ell, m=-M/2}^{M/2-1} \widetilde{v}_{\ell, m} e_{\ell, m}(\mathbf{x}),$$

where the complex exponential basis function $e_{\ell, m}(\mathbf{x}) := e^{i\nu(\ell x + m y)}$ with $\nu = 2\pi/L$. The coefficients $\widehat{v}_{\ell, m}$ refer to the standard Fourier coefficients of function $v(\mathbf{x})$, and the pseudo-spectral coefficients $\widetilde{v}_{\ell, m}$ are determined such that $(I_M v)(\mathbf{x}_h) = v_h$. The Fourier pseudo-spectral first and second order derivatives of v_h are given by

$$\mathcal{D}_x v_h := \sum_{\ell, m=-M/2}^{M/2-1} (i\nu\ell) \widetilde{v}_{\ell, m} e_{\ell, m}(\mathbf{x}_h), \quad \mathcal{D}_x^2 v_h := \sum_{\ell, m=-M/2}^{M/2-1} (i\nu\ell)^2 \widetilde{v}_{\ell, m} e_{\ell, m}(\mathbf{x}_h).$$

The operators \mathcal{D}_y and \mathcal{D}_y^2 can be defined in the similar fashion. We define the discrete gradient and Laplacian in the point-wise sense by $\nabla_h v_h := (\mathcal{D}_x v_h, \mathcal{D}_y v_h)^T$ and $\Delta_h v_h := (\mathcal{D}_x^2 + \mathcal{D}_y^2) v_h$, respectively.

For functions $v, w \in \mathbb{V}_h$, define the discrete inner product $\langle v, w \rangle := h^2 \sum_{\mathbf{x}_h \in \Omega_h} v_h w_h$, and the associated discrete L^2 norm $\|v\| := \|v\|_{l^2} = \sqrt{\langle v, v \rangle}$. Also, we will use $\|v\|_{\infty} = \max_{\mathbf{x}_h \in \Omega_h} |v_h|$, $\|\nabla_h v\| := \sqrt{h^2 \sum_{\mathbf{x}_h \in \Omega_h} |\nabla_h v_h|^2}$ and $\|\Delta_h v\| := \sqrt{h^2 \sum_{\mathbf{x}_h \in \Omega_h} |\Delta_h v_h|^2}$. It is easy to check the discrete Green's formulas, $\langle -\Delta_h v, w \rangle = \langle \nabla_h v, \nabla_h w \rangle$ and $\langle \Delta_h^2 v, w \rangle = \langle \Delta_h v, \Delta_h w \rangle$, see [6, 29] for more details. Also one has the embedding inequality simulating the Sobolev embedding $H^2(\Omega) \hookrightarrow L^{\infty}(\Omega)$,

$$\|v\|_{\infty} \leq \kappa_{\Omega} (\|v\| + \|\Delta_h v\|) \quad \text{for any } v \in \mathbb{V}_h, \quad (2.1)$$

where $\kappa_{\Omega} > 0$ is only dependent on the domain Ω_h . Here and hereafter, any subscripted κ , such as $\kappa_{\Omega}, \kappa_u, \kappa_{\phi}, \kappa_0, \kappa_1, \hat{\kappa}_1, \hat{\kappa}_1^*$ and so on, denotes a fixed constant; while any subscripted K , such as K_w and K_{ϕ} , denotes a generic positive constant, not necessarily the same at different occurrences. The appeared constants may be dependent on the given data (typically, the interface width parameter ϵ) and the solution Φ but are always independent of the spatial length h and the time-step size τ_n .

2.1 Theoretical motivation

Let $E_{s_1} := (1_{i \geq j})_{s_1 \times s_1}$ be the lower triangular matrix full of element 1, and I_{s_1} be the identity matrix of the same size as A_{Γ} . Following the derivations in [26, Section 2], one can reformulate the IERK

method (1.7) into the following differential form, also see [24, 25],

$$\sum_{\ell=1}^i d_{i\ell}(\tau_n \Delta_h L_{\kappa,h}) \delta_\tau u_h^{n,\ell+1} = \tau_n \Delta_h \left[L_{\kappa,h} u_h^{n,i+\frac{1}{2}} - f_\kappa(u_h^{n,i}) \right] \quad \text{for } n \geq 1 \text{ and } 1 \leq i \leq s_I, \quad (2.2)$$

where $\delta_\tau u_h^{n,\ell+1} := u_h^{n,\ell+1} - u_h^{n,\ell}$ for $\ell \geq 1$ is the time difference, $u_h^{n,\ell+\frac{1}{2}} := (u_h^{n,\ell+1} + u_h^{n,\ell})/2$ for $\ell \geq 1$ is the averaged operator and $d_{i\ell}$ is the element of the differentiation matrix $D = (d_{i\ell})_{s_I \times s_I}$ defined by

$$D(z) := D_E - z D_{EI} \quad \text{with} \quad D_E := A_E^{-1} E_{s_I}, \quad D_{EI} := A_E^{-1} A_I E_{s_I} - E_{s_I} + \frac{1}{2} I_{s_I}. \quad (2.3)$$

It is easy to check that the stage solutions $u_h^{n,i+1}$ of the IERK method (1.7) or (2.2) preserve the initial volume, that is,

$$\langle u^{n,i+1}, 1 \rangle = \langle u^{n,1}, 1 \rangle = \langle u^{1,1}, 1 \rangle = \langle \phi^0, 1 \rangle \quad \text{for } n \geq 1 \text{ and } 1 \leq i \leq s_I. \quad (2.4)$$

To establish the original energy dissipation law of the IERK method (2.2), we assume that the nonlinear term $F'(\Phi)$ is continuously differentiable and recall the following inequality

$$F'(u_h^{n,i})(u_h^{n,i+1} - u_h^{n,i}) \leq F(u_h^{n,i}) - F(u_h^{n,i+1}) + \frac{1}{2}(u_h^{n,i+1} - u_h^{n,i})^2 \max_{\xi_h \in \mathcal{B}_{n,i}} |F''(\xi_h)|$$

where the function space $\mathcal{B}_{n,i} := \{\xi_h \mid \|\xi\|_\infty \leq \max\{\|u^{n,i+1}\|_\infty, \|u^{n,i}\|_\infty\}\}$. By using the definitions in (1.4), it is easy to find that

$$\langle L_{\kappa,h} u^{n,i+\frac{1}{2}} - f_\kappa(u^{n,i}), \delta_\tau u^{n,i+1} \rangle \leq E[u^{n,i}] - E[u^{n,i+1}] - \frac{1}{2} \|\delta_\tau u^{n,i+1}\|^2 \left(\kappa - \max_{\xi_h \in \mathcal{B}_{n,i}} \|F''(\xi)\|_\infty \right).$$

Then by imposing the uniformly bounded assumption of stage solutions and taking the stabilized parameter $\kappa \geq \max_{\xi_h \in \mathcal{B}_{n,i}} \|F''(\xi)\|_\infty$ (the minimum size of κ would be always dependent on the regularity of initial data and the magnitude of the small interface parameter ϵ , see [14–17]), one can follow the proofs of [26, Theorem 2.1, Corollary 2.1 and Lemma 2.1] to obtain the following result. Here and hereafter, we say that a lower triangular matrix D is positive (semi-)definite if its symmetric part $\mathcal{S}(D) = (D + D^T)/2$ is positive (semi-)definite.

Lemma 2.1. *Assume that the two matrices D_E and D_{EI} in (2.3) are positive (semi-)definite. If the stage solutions $u_h^{n,\ell}$ ($n \geq 1, 1 \leq \ell \leq s$) are bounded by κ_0 in the maximum norm, and the stabilization parameter κ in (1.4) is chosen properly large such that $\kappa \geq \max_{\|\xi\|_\infty \leq \kappa_0} \|F''(\xi)\|_\infty$, then the IERK method (2.2) preserves the original energy dissipation law (1.3) at all stages,*

$$E[u^{n,i+1}] - E[u^{n,1}] \leq \frac{1}{\tau_n} \sum_{k=1}^i \left\langle \Delta_h^{-1} \delta_\tau u^{n,k+1}, \sum_{\ell=1}^k d_{k\ell}(\tau_n \Delta_h L_{\kappa,h}) \delta_\tau u^{n,\ell+1} \right\rangle \quad (2.5)$$

for $n \geq 1$ and $1 \leq i \leq s_I$. The associated average dissipation rate is nonnegative, that is,

$$\mathcal{R} = \frac{1}{s_I} \text{tr}(D_E) + \frac{1}{s_I} \text{tr}(D_{EI}) \tau_n \bar{\lambda}_{ML} = \frac{1}{s_I} \sum_{k=1}^{s_I} \frac{1}{\hat{a}_{k+1,k}} + \frac{1}{s_I} \sum_{k=1}^{s_I} \left(\frac{a_{k+1,k+1}}{\hat{a}_{k+1,k}} - \frac{1}{2} \right) \tau_n \bar{\lambda}_{ML} \geq 0, \quad (2.6)$$

where $\bar{\lambda}_{ML} > 0$ is the average eigenvalue of the symmetric, positive definite matrix $-\Delta_h L_{\kappa,h}$.

By comparing the discrete energy law (2.5) with the continuous counterpart (1.3), as remarked in [24,26], an IERK method would be a “good” candidate if the average dissipation rate \mathcal{R} is as close to 1 as possible within properly large range of $\tau_n \bar{\lambda}_{\text{ML}}$. Always, potential users will determine the value of $\tau_n \bar{\lambda}_{\text{ML}}$ by choosing the time-step size τ_n , the stabilized parameter κ , the method of spatial approximation and the spacing size h as well. *This raises an interesting question: are there any IERK methods whose average dissipation rates are independent of $\tau_n \bar{\lambda}_{\text{ML}}$?*

It has a positive answer which gives rise to a refined class of IERK method (2.2), called refined IERK (R-IERK), in which the associated average dissipation rate \mathcal{R} in (2.6) is always independent of $\tau_n \bar{\lambda}_{\text{ML}}$. Actually, from the formula (2.6), we see that \mathcal{R} is independent of $\tau_n \bar{\lambda}_{\text{ML}}$ if and only if the positive semi-definite matrix D_{EI} is a zero matrix, that is,

$$D_{\text{EI}} = A_{\text{E}}^{-1} A_{\text{I}} E_{s_{\text{I}}} - E_{s_{\text{I}}} + \frac{1}{2} I_{s_{\text{I}}} = \mathbf{0}. \quad (2.7)$$

It can be achieved by taking $A_{\text{I}} := A_{\text{E}} P_{s_{\text{I}}}$ with $P_{s_{\text{I}}} := I_{s_{\text{I}}} - \frac{1}{2} E_{s_{\text{I}}}^{-1}$. In such case, the differentiation matrix $D(z)$ in (2.3) is independent of z , that is,

$$D_{\text{R}} := (d_{ij}^{(R)})_{s_{\text{I}} \times s_{\text{I}}} = D_{\text{E}} = A_{\text{E}}^{-1} E_{s_{\text{I}}}, \quad (2.8)$$

and the associated average dissipation rate \mathcal{R} in (2.6) is reduced into

$$\mathcal{R}_{\text{R}} := \frac{1}{s_{\text{I}}} \sum_{k=1}^{s_{\text{I}}} \frac{1}{\hat{a}_{k+1,k}}. \quad (2.9)$$

The IERK scheme (1.7) reduces into the following R-IERK method

$$u_h^{n,i+1} = u_h^{n,1} + \tau_n \sum_{j=1}^i \hat{a}_{i+1,j} \Delta_h \left[L_{\kappa,h} u_h^{n,j+\frac{1}{2}} - f_{\kappa}(u_h^{n,j}) \right] \quad \text{for } n \geq 1 \text{ and } 1 \leq i \leq s_{\text{I}}, \quad (2.10)$$

or, with the matrix $(\hat{a}_{i+1,j})_{s_{\text{I}} \times s_{\text{I}}} := E_{s_{\text{I}}}^{-1} A_{\text{E}}$,

$$\delta_{\tau} u_h^{n,i+1} = \tau_n \sum_{j=1}^i \hat{a}_{i+1,j} \Delta_h \left[L_{\kappa,h} u_h^{n,j+\frac{1}{2}} - f_{\kappa}(u_h^{n,j}) \right] \quad \text{for } n \geq 1 \text{ and } 1 \leq i \leq s_{\text{I}}. \quad (2.11)$$

The implicit part of the IERK method (2.2) will be completely determined by its explicit part. It means that more stages and computational cost would be required to achieve the interesting property (2.7) of R-IERK methods due to the vanish of the degree of freedom in the implicit part. According to the canopy node condition, $\hat{\mathbf{c}} = \mathbf{c}$ or $\mathbf{A}\mathbf{1} = \hat{\mathbf{A}}\mathbf{1}$, it is not difficult to compute the coefficient vector of the first column, $\mathbf{a}_1 = (\frac{1}{2}\hat{a}_{21}, \frac{1}{2}\hat{a}_{31}, \dots, \frac{1}{2}\hat{a}_{s_{\text{I}}1})^T$. As seen, the implicit part of the R-IERK method (2.10) allows a stage-order of two so that it would be not necessarily algebraically stable, cf. [12,33]. Moreover, the non-zero vector \mathbf{a}_1 implies the following result because the Radau-type or ARS-type IERK methods always require $\mathbf{a}_1 = \mathbf{0}$, see [2,3,8].

Proposition 2.1. *There are no Radau-type or ARS-type IERK methods that the associated average dissipation rates are independent of the time-space discretization parameter $\tau_n \bar{\lambda}_{\text{ML}}$.*

2.2 Numerical motivation

Before we turn to high-order R-IERK methods, some preliminary tests are presented to show the advantage of R-IERK methods in self-adaptive computations. Consider the IERK(1,2; θ) method

$$\begin{array}{c|c} \mathbf{c} & A \\ \hline & \mathbf{b}^T \end{array} = \frac{0}{1} \left| \begin{array}{cc} 0 & 0 \\ 1-\theta & \theta \\ 1-\theta & \theta \end{array} \right., \quad \begin{array}{c|c} \hat{\mathbf{c}} & \hat{A} \\ \hline & \hat{\mathbf{b}}^T \end{array} = \frac{0}{1} \left| \begin{array}{cc} 0 & 0 \\ 1 & 0 \\ 1 & 0 \end{array} \right|. \quad (2.12)$$

Obviously, $A_I = (\theta)$ and $A_E = (1)$ such that the differentiation matrix $D^{(1,2)}(z) = 1 - z(\theta - \frac{1}{2})$ is positive definite for $z \leq 0$ provided $\theta \geq \frac{1}{2}$ according to Lemma 2.1. The average dissipation rate

$$\mathcal{R}^{(1,2)}(\theta) = 1 + (\theta - \frac{1}{2}) \tau_n \bar{\lambda}_{ML} \quad \text{for } \theta \geq \frac{1}{2}. \quad (2.13)$$

Choosing the weighted parameter $\theta = 1/2$, we have $\mathcal{R}_R^{(1,2)} = \mathcal{R}^{(1,2)}(\frac{1}{2}) = 1$, which is independent of $\tau_n \bar{\lambda}_{ML}$, and the associated Crank-Nicolson-type R-IERK(1,2) scheme,

$$\delta_\tau \phi_h^n = \tau_n \Delta_h \left[\frac{1}{2} L_{\kappa,h}(\phi_h^n + \phi_h^{n-1}) - f_\kappa(\phi_h^{n-1}) \right] \quad \text{for } n \geq 1.$$

Example 1. Consider the Cahn-Hilliard model (1.2) on the spatial domain $\Omega = (-\pi, \pi)^2$ with the interface parameter $\epsilon = 0.1$, subject to the initial data

$$\Phi^0 = \frac{1}{2} \tanh(|x| + |y| + 1) - e^{-5(|x|+|y|-2)^2} + \frac{1}{2} e^{-2(|x|-1)^2} + \frac{1}{10} \sin(e^{|y|-1}).$$

The reference solution is generated with $\tau = 10^{-4}$ by the Lobatto-type IERK2-2 method in [26] for the parameter $a_{33} = \frac{1+\sqrt{2}}{4}$, called IERK(2,3) method hereafter, which is regarded as the best one among second-order IERK methods in [26] with the associated average dissipation rate $\mathcal{R}_L^{(2,3)} = \sqrt{2} + \frac{\sqrt{2}}{4} \tau_n \bar{\lambda}_{ML}$.

To investigate the energy behavior in adaptive time-stepping calculation, we always choose the adaptive step-size [10, 23], $\tau_{ada} = \max\{\tau_{\min}, \tau_{\max}/\Pi_\eta(\phi)\}$ with $\Pi_\eta(\phi) := \sqrt{1 + \eta \|\partial_\tau \phi^n\|^2}$, where τ_{\max} and τ_{\min} refer to the predetermined maximum and minimum time-step sizes, and η is chosen by the user to adjust the level of adaptivity. Hereafter, if not explicitly specified, we set the adaptivity parameter $\eta = 1000$, the minimum step $\tau_{\min} = 10^{-4}$ and the initial step size $\tau_1 = \tau_{\min}$.

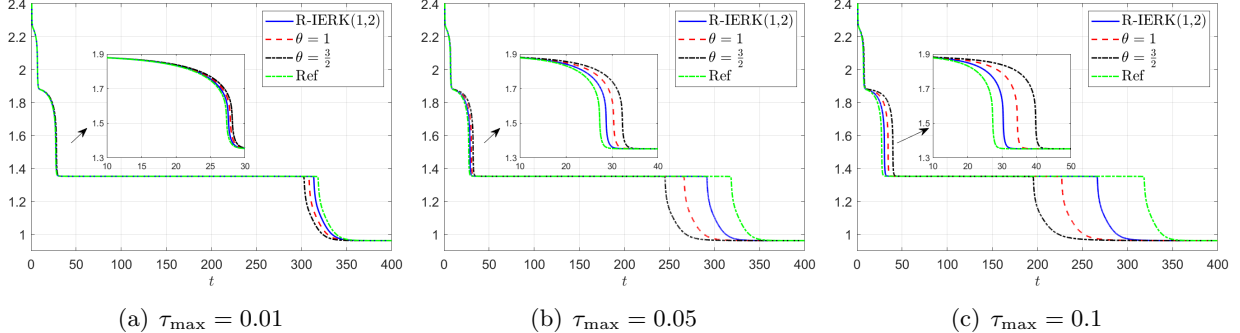


Figure 1: Energy behaviors of R-IERK(1,2) method and IERK(1,2; θ) method (2.12).

We run the R-IERK(1,2) method and the IERK(1,2; θ) method (2.12) with the stabilized parameter $\kappa = 2.5$ to the final time $T = 1000$. Figure 1 depicts the discrete energy curves (the discrete energies over $t \in [400, 1000]$ are unchanged and omitted here to display the rapidly changing parts more finely) for three different scenes: (a) $\tau_{\max} = 0.01$, (b) $\tau_{\max} = 0.05$ and (c) $\tau_{\max} = 0.1$. Under the same time-adaptive strategy with different maximum time step τ_{\max} , the energy curves of the R-IERK(1,2) method are always closer to the reference energy than those of the IERK(1,2; θ) methods with $\theta = 1$ and $\frac{3}{2}$. The IERK(1,2; θ) methods with $\theta = 1$ and $\frac{3}{2}$ seem more susceptible with respect to the change of time-step sizes; while the R-IERK(1,2) method allows some larger adaptive step-sizes and would be more preferable in adaptive numerical simulations. This phenomenon would be attributed to the constant rate of average dissipation rate, $\mathcal{R}_R^{(1,2)} = 1$, which is independent of the time-space discretization parameter $\tau_n \bar{\lambda}_{ML}$.

3 Construction of parameterized R-IERK methods

3.1 Second-order R-IERK methods

Second-order R-IERK methods require two implicit stages, $s_I = 2$, at least; however, it is easy to check that no 3-stage R-IERK method exists for second-order accuracy.

We turn to consider 4-stage R-IERK methods that satisfy the canopy node condition and the first-order conditions in Table 1,

$$\mathbf{c} \left| \begin{array}{c} A \\ \mathbf{b}^T \end{array} \right. = \begin{array}{c|ccc} 0 & 0 & & \\ c_2 & \frac{c_2}{2} & \frac{c_2}{2} & \\ c_3 & \frac{c_3 - c_2}{2} & \frac{c_3}{2} & \frac{c_2}{2} \\ 1 & \frac{1 - \hat{a}_{42} - c_2}{2} & \frac{1 - c_2}{2} & \frac{\hat{a}_{42} + c_2}{2} \quad \frac{c_2}{2} \\ \hline & \frac{1 - \hat{a}_{42} - c_2}{2} & \frac{1 - c_2}{2} & \frac{\hat{a}_{42} + c_2}{2} \quad \frac{c_2}{2} \end{array}, \quad \hat{\mathbf{c}} \left| \begin{array}{c} \hat{A} \\ \hat{\mathbf{b}}^T \end{array} \right. = \begin{array}{c|ccc} 0 & 0 & & \\ c_2 & c_2 & 0 & \\ c_3 & c_3 - c_2 & c_2 & 0 \\ 1 & 1 - \hat{a}_{42} - c_2 & \hat{a}_{42} & c_2 \quad 0 \\ \hline & 1 - \hat{a}_{42} - c_2 & \hat{a}_{42} & c_2 \quad 0 \end{array},$$

where we set $\hat{a}_{32} := c_2$ and $\hat{a}_{43} := c_2$ to reduce the degree of freedom and there are three independent coefficients c_2 , c_3 and \hat{a}_{42} . These simplifying settings are also useful for practical applications since they provide a constant iteration matrix for the system of linear equations at all stages. According to the stand-alone conditions for second-order accuracy, $\hat{\mathbf{b}}^T \mathbf{c} = \frac{1}{2}$ and $\mathbf{b}^T \mathbf{c} = \frac{1}{2}$, one has

$$\hat{a}_{42} = \frac{1}{2c_2} - c_3 \quad \text{and} \quad (1 - c_2)c_2 + (\hat{a}_{42} + c_2)c_3 + c_2 = 1.$$

They reduce into the quadratic equation, $c_3^2 - (\frac{1}{2c_2} + c_2)c_3 + (c_2 - 1)^2 = 0$. If $0 < c_2 \leq \frac{2+\sqrt{6}}{2}$ such that $2c_2^2 - 4c_2 - 1 \leq 0$, one gets

$$c_3^* := \frac{3}{2} \quad \text{if } c_2 = 1 \quad \text{and} \quad c_3^* := \frac{1}{4c_2} + \frac{c_2}{2} - \frac{\sqrt{(-2c_2^2 + 4c_2 + 1)(6c_2^2 - 4c_2 + 1)}}{4c_2} > 0 \quad \text{if } c_2 \neq 1, \quad (3.1)$$

where the other positive root $c_3 = \frac{1}{4c_2} + \frac{c_2}{2} + \frac{\sqrt{(-2c_2^2 + 4c_2 + 1)(6c_2^2 - 4c_2 + 1)}}{4c_2}$ is dropped for $c_2 \neq 1$.

By using the definition in (2.8), one has

$$D_{\mathbf{R}}^{(2,4)}(c_2) = \begin{pmatrix} \frac{1}{c_2} & 0 & 0 \\ \frac{2c_2 - c_3^*}{c_2^2} & \frac{1}{c_2} & 0 \\ \frac{4c_2^3 - 2c_2^2 - c_2 + 2c_2^2 c_3^* + c_3^* - 2c_2(c_3^*)^2}{2c_2^4} & \frac{2c_2^2 + 2c_3^* c_2 - 1}{2c_2^3} & \frac{1}{c_2} \end{pmatrix}.$$

Now consider the positive definiteness of $D_{\mathbf{R}}^{(2,4)}(c_2)$. It is easy to check that the first leading principal minor is positive, the second principal minor $\text{Det}[\mathcal{S}(D_{\mathbf{R},2}^{(2,4)}; c_2)] = \frac{c_3(4c_2 - c_3)}{4c_2^4} > 0$ for $0 < c_2 \leq \frac{2+\sqrt{6}}{2}$, while $\text{Det}[\mathcal{S}(D_{\mathbf{R}}^{(2,4)}; c_2)] = \frac{1}{8c_2^2}(c_2 - 1)^2(2c_2^2 + 2c_2 - 1) > 0$ for $c_2 \geq \frac{\sqrt{3}-1}{2}$ and $c_2 \neq 1$. Thus the differentiation matrix $D_{\mathbf{R}}^{(2,4)}(c_2)$ is positive definite if $\frac{\sqrt{3}-1}{2} \leq c_2 < 1$ or $1 < c_2 \leq \frac{2+\sqrt{6}}{2}$. We obtain the one-parameter R-IERK(2,4; c_2) methods with the associated Butcher tableaux

$$\begin{array}{c|ccc} 0 & 0 & & \\ c_2 & \frac{c_2}{2} & \frac{c_2}{2} & \\ c_3^* & \frac{c_3^* - c_2}{2} & \frac{c_3^*}{2} & \frac{c_2}{2} \\ 1 & \frac{1 + c_3^* - c_2}{2} - \frac{1}{4c_2} & \frac{1 - c_2}{2} & \frac{1}{4c_2} + \frac{c_2 - c_3^*}{2} \quad \frac{c_2}{2} \\ \hline & \frac{1 + c_3^* - c_2}{2} - \frac{1}{4c_2} & \frac{1 - c_2}{2} & \frac{1}{4c_2} + \frac{c_2 - c_3^*}{2} \quad \frac{c_2}{2} \end{array}, \quad \begin{array}{c|ccc} 0 & 0 & & \\ c_2 & c_2 & 0 & \\ c_3^* & c_3^* - c_2 & c_2 & 0 \\ 1 & 1 - \frac{1}{2c_2} + c_3^* - c_2 & \frac{1}{2c_2} - c_3^* & c_2 \quad 0 \\ \hline & 1 - \frac{1}{2c_2} + c_3^* - c_2 & \frac{1}{2c_2} - c_3^* & c_2 \quad 0 \end{array}, \quad (3.2)$$

where c_3^* is defined by (3.1). The associated average dissipation rate is

$$\mathcal{R}_{\mathbf{R}}^{(2,4)}(c_2) = \text{tr}[D_{\mathbf{R}}^{(2,4)}(c_2)] = \frac{1}{c_2} \quad \text{for } \frac{\sqrt{3}-1}{2} \leq c_2 < 1 \text{ or } 1 < c_2 \leq \frac{2+\sqrt{6}}{2}. \quad (3.3)$$

Remark 1. The case $c_2 = 1$ in (3.3) will arrive at $\mathcal{R}_R^{(2,4)}(1) = 1$, the optimal value of average dissipation rate. It is noticed that the symmetric matrix $\mathcal{S}(D_R^{(2,4)}; 1)$ is singular since $\text{Det}[\mathcal{S}(D_R^{(2,4)}; 1)] = 0$. This case is permitted in Lemma 2.1, which is valid under the global Lipschitz continuity assumption of nonlinear bulk, cf. [26, Theorem 2.1 and Corollary 2.1]; however, this case should be excluded in our current discussions because it does not fulfill the conditions of Lemma 4.3 and Theorems 4.1-4.3, which require that the symmetric part $\mathcal{S}(D_R^{(2,4)}(c_2))$ has a finite minimum eigenvalue $\lambda_{\min} > 0$. It is to mention that, the corresponding R-IERK(2,4;1) scheme still performs well in our numerical experiments, see Section 5, although we cannot theoretically verify the stability and convergence yet.

3.2 Third-order R-IERK methods

It is not difficult to check that no 4-stage R-IERK method exists for the third-order accuracy. One can consider the five-stage R-IERK method which has only nine independent coefficients. From Table 1, eight order conditions are required such that there remains one independent variable. Unfortunately, we are not able to find any third-order R-IERK methods within five stages to ensure the positive (semi-)definite of the corresponding differentiation matrix $D_R = D_E$.

We consider six-stage method with one free variable \hat{a}_{52} by choosing $c_2 = 1$, $c_3 = \frac{4}{5}$, $c_4 = \frac{7}{10}$, $c_5 = \frac{12}{25}$ and $\hat{a}_{32} = \frac{6}{5}$ after a trial and error process. It arrives at one-parameter R-IERK(3,6; \hat{a}_{52}) methods with the following Butcher tableaux

$$\begin{array}{c|cccccc} 0 & 0 & & & & \\ 1 & \frac{1}{2} & \frac{1}{2} & & & \\ \frac{4}{5} & -\frac{1}{5} & \frac{2}{5} & \frac{3}{5} & & \\ \mathbf{c} \mid \hat{A} & \frac{7}{10} & -\frac{98716201}{329771428} & -\frac{2367068609}{14839714260} & \frac{267670251}{412214285} & \frac{378048430}{741985713} \\ \mid \mathbf{b}^T & \frac{12}{25} & \frac{1}{2}\hat{a}_{51} & \frac{\hat{a}_{51}+\hat{a}_{52}}{2} & \frac{\hat{a}_{52}+\hat{a}_{53}}{2} & \frac{\hat{a}_{53}+\hat{a}_{54}}{2} & \frac{35\hat{a}_{52}}{103} + \frac{89552314349}{363926325900} \\ 1 & \frac{206221}{2306412} & \frac{355973}{1153206} & -\frac{422005}{768804} & \frac{13730}{192201} & \frac{553250}{576603} & \frac{69125}{576603} \end{array}, \quad (3.4a)$$

$$\begin{array}{c|cccccc} 0 & 0 & & & & \\ 1 & 1 & 0 & & & \\ \frac{4}{5} & -\frac{2}{5} & \frac{6}{5} & 0 & & \\ \hat{\mathbf{c}} \mid \hat{A} & \frac{7}{10} & -\frac{98716201}{164885714} & \frac{1037580218}{3709928565} & \frac{756096860}{741985713} & 0 \\ \mid \hat{\mathbf{b}}^T & \frac{12}{25} & \hat{a}_{51} & \hat{a}_{52} & \frac{14091138538}{30327193825} - \frac{190\hat{a}_{52}}{103} & \frac{70\hat{a}_{52}}{103} + \frac{89552314349}{181963162950} & 0 \\ 1 & \frac{206221}{1153206} & \frac{168575}{384402} & -\frac{98430}{64067} & \frac{322750}{192201} & \frac{138250}{576603} & 0 \\ & \frac{206221}{1153206} & \frac{168575}{384402} & -\frac{98430}{64067} & \frac{322750}{192201} & \frac{138250}{576603} & 0 \end{array}, \quad (3.4b)$$

where the coefficient $\hat{a}_{51} = \frac{17\hat{a}_{52}}{103} - \frac{86756827361}{181963162950}$. Simple calculations yield the differentiation matrix $D_R^{(3,6)}(\hat{a}_{52}) = A_E^{-1}(\hat{a}_{52})E_5$, which is always positive definite if $0.664767 < \hat{a}_{52} < 0.751947$. The associated average dissipation rate reads

$$\mathcal{R}_R^{(3,6)}(\hat{a}_{52}) = \frac{36392632590}{123664285500\hat{a}_{52}+89552314349} + \frac{219055887768899}{156795586342500} \approx \frac{1.39708\hat{a}_{52}+1.30599}{\hat{a}_{52}+0.724157}. \quad (3.5)$$

We are not sure whether there exists a six-stage IERK scheme having the optimal value of average dissipation rate, $\mathcal{R}_R^{(3,6)} = 1$. Here we do not attempt to construct a fourth-order R-IERK method. Actually, the large number (twenty-eight) of order conditions, cf. [2, 11, 26], makes the fourth-order R-IERK method require at least nine stages so that it would be computationally intensive.

4 Energy dissipation laws and L^2 norm convergence

4.1 Technical lemmas and time-discrete system

We use the standard seminorms and norms in the Sobolev space $H^m(\Omega)$ for $m \geq 0$. Let $C^\infty(\Omega)$ be a set of infinitely differentiable L -periodic functions defined on Ω , and $H_{per}^m(\Omega)$ be the closure of $C^\infty(\Omega)$ in $H^m(\Omega)$, endowed with the semi-norm $|\cdot|_{H_{per}^m}$ and the norm $\|\cdot\|_{H_{per}^m}$. For simplicity, denote $|\cdot|_{H^m} := |\cdot|_{H_{per}^m}$, $\|\cdot\|_{H^m} := \|\cdot\|_{H_{per}^m}$, $\|\cdot\|_{L^2} := \|\cdot\|_{H^0}$, and the maximum norm $\|\cdot\|_{L^\infty}$.

Next lemma lists some approximations of the L^2 -projection operator P_M and trigonometric interpolation operator I_M defined in subsection 2.1.

Lemma 4.1. [29] *For any $w \in H_{per}^q(\Omega)$ and $0 \leq \ell \leq q$, it holds that*

$$\|P_M w - w\|_{H^\ell} \leq K_w h^{q-s} |w|_{H^q}, \quad \|P_M w\|_{H^\ell} \leq K_w \|w\|_{H^\ell};$$

and, in addition if $q > 3/2$,

$$\|I_M w - w\|_{H^\ell} \leq K_w h^{q-\ell} |w|_{H^q}, \quad \|I_M w\|_{H^\ell} \leq K_w \|w\|_{H^\ell}.$$

In deriving the stability and error estimate of the stage solutions for semi-implicit multi-stage methods, we need the following Grönwall-type lemma.

Lemma 4.2. *For any integers $s > 1$ and $N > 1$, let $v_{n,i}$, $g_{n,i}$ and $\tilde{g}_{n,i}$ be the nonnegative discrete functions defined at the stage $t_{n,i}$ for the time level indexes $n = 1, 2, \dots, N$ and the stage indexes $i = 1, 2, \dots, s$ with a finite $T = t_N = t_{N,s}$. Also, let $v_n := v_{n,s} = v_{n+1,1}$. Assume further that $g_{n,i}$ and $\tilde{g}_{n,i}$ are bounded for $1 \leq i \leq s$ and $n \geq 1$. There exists a positive constant ω_0 , independent of the time-step sizes τ_n , such that*

$$v_{n,i} \leq v_{n,1} + \omega_0 \tau_n \sum_{j=1}^{i-1} v_{n,j} + \sum_{j=2}^i g_{n,j} + \tilde{g}_{n,i} \quad \text{for } n \geq 1 \text{ and } 2 \leq i \leq s. \quad (4.1)$$

If the maximum step-size τ is small such that $\tau \leq 1/\omega_0$, it holds that

$$v_{n,i} \leq 4^{s-1} \exp(2^{s-1} \omega_0 t_{n-1}) \left(v_0 + \sum_{k=1}^{n-1} \sum_{j=2}^s g_{k,j} + \sum_{j=2}^i g_{n,j} + \sum_{k=1}^n \max_{2 \leq j \leq s} \tilde{g}_{k,j} \right)$$

for $1 \leq n \leq N$ and $2 \leq i \leq s$.

Proof. For fixed n , a simple induction for (4.1) gives the stage estimate

$$v_{n,i} \leq (1 + \omega_0 \tau_n)^{i-1} \left(v_{n,1} + \sum_{\ell=2}^i g_{n,\ell} + \max_{2 \leq j \leq s} \tilde{g}_{n,j} \right) \quad (4.2)$$

for $2 \leq i \leq s$. Taking $i = s$ and $n = k$ in the inequality (4.1) yields

$$v_k = v_{k,s} \leq v_{k-1} + \omega_0 \tau_k \sum_{j=1}^{s-1} v_{k,j} + \sum_{j=2}^s g_{k,j} + \tilde{g}_{k,s} \quad \text{for } k \geq 1, \quad (4.3)$$

and, by summing the index k from 1 to n ,

$$v_n \leq v_0 + \omega_0 \sum_{k=1}^n \sum_{j=1}^{s-1} \tau_k v_{k,j} + \sum_{k=1}^n \sum_{j=2}^s g_{k,j} + \sum_{k=1}^n \tilde{g}_{k,s} \quad \text{for } n \geq 1.$$

Now we insert the stage estimate (4.2) into the above inequality to obtain that

$$\begin{aligned}
v_n &\leq (1 + \omega_0 \tau_1)^{s-1} v_0 + \omega_0 \sum_{k=2}^n \tau_k v_{k-1} \sum_{j=1}^{s-1} (1 + \omega_0 \tau_k)^{j-1} \\
&\quad + \sum_{k=1}^n (1 + \omega_0 \tau_k)^{s-1} \sum_{j=2}^s g_{k,j} + \sum_{k=1}^n (1 + \omega_0 \tau_k)^{s-1} \max_{2 \leq j \leq s} \tilde{g}_{k,j}
\end{aligned} \tag{4.4}$$

for $n \geq 1$, where we used the facts $g_{k,j} \geq 0$, $\tilde{g}_{k,j} \geq 0$ and $1 + \omega_0 \tau_k \sum_{j=1}^{s-1} (1 + \omega_0 \tau_k)^{j-1} = (1 + \omega_0 \tau_k)^{s-1}$. Under the maximum step-size setting $\tau \leq 1/\omega_0$, one has

$$(1 + \omega_0 \tau_k)^{s-1} \leq 2^{s-1} \quad \text{and} \quad \sum_{j=1}^{s-1} (1 + \omega_0 \tau_k)^{j-1} \leq \sum_{j=1}^{s-1} 2^{j-1} = 2^{s-1} - 1.$$

It follows from (4.4) that

$$v_n \leq 2^{s-1} v_0 + 2^{s-1} \omega_0 \sum_{k=2}^n \tau_k v_{k-1} + 2^{s-1} \sum_{k=1}^n \sum_{j=2}^s g_{k,j} + 2^{s-1} \sum_{k=1}^n \max_{2 \leq j \leq s} \tilde{g}_{k,j} \quad \text{for } n \geq 1.$$

The discrete Grönwall inequality, cf. [27, Lemma 3.1], leads to the time-level estimate,

$$v_n \leq 2^{s-1} \exp(2^{s-1} \omega_0 t_n) \left(v_0 + \sum_{k=1}^n \sum_{j=2}^s g_{k,j} + \sum_{k=1}^n \max_{2 \leq j \leq s} \tilde{g}_{k,j} \right) \quad \text{for } 1 \leq n \leq N.$$

Return to the stage estimate (4.2) with the setting $\tau \leq 1/\omega_0$, we get the time-stage estimate

$$v_{n,i} \leq 4^{s-1} \exp(2^{s-1} \omega_0 t_{n-1}) \left(v_0 + \sum_{k=1}^{n-1} \sum_{j=2}^s g_{k,j} + \sum_{j=2}^i g_{n,j} + \sum_{k=1}^{n-1} \max_{2 \leq j \leq s} \tilde{g}_{k,j} + \max_{2 \leq i \leq s} \tilde{g}_{n,j} \right)$$

for $1 \leq n \leq N$ and $1 \leq i \leq s$. It completes the proof. \square

To establish the original energy dissipation laws and the L^2 norm error estimate of the fully discrete R-IERK method (2.10) for the fourth-order nonlinear CH model, we will update the idea of time-space error splitting approach in [18, 19] via the following three steps:

(Step 1) Subsection 4.2 addresses the time-discrete system to establish the regularity of time-discrete stage solutions $U^{n,i}$ via the energy arguments with a rough setting of stage defects. Always, we assume that the initial data and the solution of (1.2) are smooth. There exist two integers $m \geq 1$, $p \geq 1$ and a constant $K_\phi > 0$ such that

$$\|\Phi^0\|_{H^{m+4}} + \sum_{k=0}^2 \|\partial_t^{(k)} \Phi(t)\|_{H^{m+4-k}} + \sum_{k=3}^{p+1} \|\partial_t^{(k)} \Phi(t)\|_{L^2} \leq K_\phi \quad \text{for } 0 < t < T. \tag{4.5}$$

(Step 2) Subsection 4.3 addresses the fully-discrete L^2 norm error estimate by using the pseudo-spectral approximation of time-discrete system and establishes the maximum norm boundedness of stage solutions $u_h^{n,i}$ via the inverse estimate such that we can establish the original energy dissipation law of the fully discrete R-IERK method (2.10).

(Step 3) With the established regularity of time-discrete solution and the maximum norm boundedness of stage solutions, Subsection 4.4 arrives at the L^2 norm error estimate for the fully discrete R-IERK method (2.10) with the full accuracy.

To process the numerical analysis of the fully discrete R-IERK method (2.10), we will consider time-discrete stage solution $U^{n,i}$ satisfying the following time-discrete system

$$U^{n,i+1} = U^{n,1} + \tau_n \sum_{j=1}^i \hat{a}_{i+1,j} \Delta \left[L_\kappa U^{n,j+\frac{1}{2}} - f_\kappa(U^{n,j}) \right] \quad \text{for } n \geq 1 \text{ and } 1 \leq i \leq s_I, \quad (4.6)$$

subject to the initial data $U^{1,1} = \Phi^{1,1} := \Phi(\mathbf{x}, 0)$. Inserting the exact solution at the stage $t_{n,i}$, $\Phi^{n,i} := \Phi(\mathbf{x}, t_{n-1} + c_i \tau_n)$, into the time-discrete system, one has

$$\Phi^{n,i+1} = \Phi^{n,1} + \tau_n \sum_{j=1}^i \hat{a}_{i+1,j} \Delta \left[L_\kappa \Phi^{n,j+\frac{1}{2}} - f_\kappa(\Phi^{n,j}) \right] + \tau_n \zeta_{\mathbb{R}}^{n,i+1} \quad \text{for } n \geq 1 \text{ and } 1 \leq i \leq s_I, \quad (4.7)$$

where the temporal defects $\zeta_{\mathbb{R}}^{n,i+1}$ at the stage $t_{n,i+1}$ will be determined later (with $\zeta_{\mathbb{R}}^{n,1} \equiv 0$). The time errors $\tilde{U}^{n,i+1} := \Phi^{n,i+1} - U^{n,i+1}$ fulfill the time-error system

$$\tilde{U}^{n,i+1} = \tilde{U}^{n,1} + \tau_n \sum_{j=1}^i \hat{a}_{i+1,j} \Delta \left[L_\kappa \tilde{U}^{n,j+\frac{1}{2}} + f_\kappa(U^{n,j}) - f_\kappa(\Phi^{n,j}) \right] + \tau_n \zeta_{\mathbb{R}}^{n,i+1}, \quad (4.8)$$

or, with the matrix $(\hat{a}_{i+1,j})_{s_I \times s_I} = E_{s_I}^{-1} A_E = D_{\mathbb{R}}^{-1}$,

$$\delta_\tau \tilde{U}^{n,i+1} = \tau_n \sum_{j=1}^i \hat{a}_{i+1,j} \Delta \left[L_\kappa \tilde{U}^{n,j+\frac{1}{2}} + f_\kappa(U^{n,j}) - f_\kappa(\Phi^{n,j}) \right] + \tau_n \delta_\tau \zeta_{\mathbb{R}}^{n,i+1} \quad (4.9)$$

for $n \geq 1$ and $1 \leq i \leq s_I$. Note that, the exact solution $\Phi^{n,i}$ and the time-discrete solution $U^{n,i}$ preserve the volume conservation such that $(\tilde{U}^{n,i}, 1) = 0$ and $(\zeta_{\mathbb{R}}^{n,i}, 1) = 0$ for $n \geq 1$ and $1 \leq i \leq s$. Recalling the orthogonal property, cf. [26, subsection 2.1], one has

$$\sum_{i=1}^k d_{k,i}^{(R)} \sum_{j=1}^i \hat{a}_{i+1,j} v^j = \sum_{j=1}^k v^j \sum_{i=j}^k d_{k,i}^{(R)} \hat{a}_{i+1,j} \equiv v^k \quad \text{for } 1 \leq k \leq s_I.$$

Multiplying both sides of the equality (4.9) by the kernels $d_{j,i}^{(R)}$ defined in (2.8), and summing the stage index i from $i = 1$ to j , it is easy to obtain the following equivalent form of (4.9),

$$\sum_{i=1}^j d_{j,i}^{(R)} \delta_\tau \tilde{U}^{n,i+1} = \tau_n \Delta \left[L_\kappa \tilde{U}^{n,j+\frac{1}{2}} + f_\kappa(U^{n,j}) - f_\kappa(\Phi^{n,j}) \right] + \tau_n \sum_{i=1}^j d_{j,i}^{(R)} \delta_\tau \zeta_{\mathbb{R}}^{n,i+1} \quad (4.10)$$

for $n \geq 1$ and $1 \leq j \leq s_I$.

It is to mention that, the time-error system (4.9) will be used for the L^2 norm estimate of stage solution; while the equivalent form (4.10) will be used for the H_{per}^2 seminorm estimate. To treat with the involved method coefficients $\hat{a}_{i+1,j}$ and $d_{i,j}^{(R)}$, we will use the following lemma.

Lemma 4.3. *Assume that the differentiation matrix $D_{\mathbb{R}} = A_E^{-1} E_{s_I}$ of the R-IERK method (2.10) and the inverse $D_{\mathbb{R}}^{-1}$ are positive definite. Let λ_{\min} and σ_{\min} be the minimum eigenvalues of the symmetric parts $\mathcal{S}(D_{\mathbb{R}})$ and $\mathcal{S}(D_{\mathbb{R}}^{-1})$, respectively. Then, for any time sequences $\{v^j, u^j \mid j \geq 1\}$, it holds that*

$$(i) \sum_{i=1}^k \sum_{j=1}^i d_{i,j}^{(R)} v^j v^i \geq \lambda_{\min} \sum_{i=1}^k (v^i)^2, \quad \text{and} \quad \sum_{i=1}^k \sum_{j=1}^i \hat{a}_{i+1,j} v^j v^i \geq \sigma_{\min} \sum_{i=1}^k (v^i)^2;$$

$$(ii) \sum_{i=1}^k \sum_{j=1}^i d_{i,j}^{(R)} v^j u^i \leq \frac{1}{\sigma_{\min}} \sum_{i=1}^k |v^i| |u^i|, \quad \text{and} \quad \sum_{i=1}^k \sum_{j=1}^i \hat{a}_{i+1,j} v^j u^i \leq \frac{1}{\lambda_{\min}} \sum_{i=1}^k |v^i| |u^i|.$$

Proof. The result (i) is obvious. Since $D_R - \lambda_{\min} I$ is positive semi-definite, [5, Lemma 5.2] says that the maximum eigenvalue of $(D_R^{-1})^T D_R^{-1}$ can be bounded by $1/\lambda_{\min}^2$. Similarly, the maximum eigenvalue of $D_R^T D_R$ can be bounded by $1/\sigma_{\min}^2$. They imply the result (ii) and complete the proof. \square

In handling the nonlinear term, the following technical lemma will be helpful, while the proof is simple due to the formula $F'(v) - F'(w) = (v - w) \int_0^1 F''[\gamma v + (1 - \gamma)w] d\gamma$. Actually, it is easy to derive that $F'(\Phi^{n,j}) - F'(U^{n,j}) = \tilde{U}^{n,j} \int_0^1 F''(U^{n,j} + \gamma \tilde{U}^{n,j}) d\gamma$, and

$$\begin{aligned} \delta_\tau F'(\Phi^{n,j}) - \delta_\tau F'(U^{n,j}) &= \delta_\tau \tilde{U}^{n,j} \int_0^1 F''(U^{n,j-1} + \beta \delta_\tau U^{n,j}) d\beta \\ &\quad + \delta_\tau \Phi^{n,j} \int_0^1 (\tilde{U}^{n,j-1} + \beta \delta_\tau \tilde{U}^{n,j}) \int_0^1 F'''[U^{n,j-1} + \beta \delta_\tau U^{n,j} + \gamma(\tilde{U}^{n,j-1} + \beta \delta_\tau \tilde{U}^{n,j})] d\gamma d\beta, \end{aligned}$$

where $\delta_\tau \Phi^{n,j} = (t_{n,j} - t_{n,j-1}) \int_0^1 \frac{d}{dt} \Phi[t_{n,j-1} + \beta(t_{n,j} - t_{n,j-1})] d\beta$.

Lemma 4.4. *Under the regularity setting (4.5), it holds that*

$$(i) \quad \|F'(\Phi^{n,j}) - F'(U^{n,j})\|_{L^2} \leq \|\tilde{U}^{n,j}\|_{L^2} \int_0^1 \|F''(\mathcal{Q}_\gamma^{n,j}[U])\|_{L^\infty} d\gamma, \quad \text{where } \mathcal{Q}_\gamma^{n,j}[U] := U^{n,j} + \gamma \tilde{U}^{n,j};$$

$$(ii) \quad \|\delta_\tau \Phi^{n,j}\|_{L^\infty} \leq |t_{n,j} - t_{n,j-1}| \|\partial_t \Phi(t)\|_{L^\infty} \leq K_\phi \tau_n \quad \text{and then}$$

$$\begin{aligned} \|\delta_\tau F'(\Phi^{n,j}) - \delta_\tau F'(U^{n,j})\|_{L^2} &\leq \|\delta_\tau \tilde{U}^{n,j}\|_{L^2} \int_0^1 \|F''(\mathcal{Q}_\beta^{n,j}[U])\|_{L^\infty} d\beta \\ &\quad + 2K_\phi \tau_n (\|\tilde{U}^{n,j}\|_{L^2} + \|\tilde{U}^{n,j-1}\|_{L^2}) \int_0^1 \int_0^1 \|F'''(\mathcal{Q}_{\beta,\gamma}^{n,j}[U])\|_{L^\infty} d\gamma d\beta, \end{aligned}$$

where $\mathcal{Q}_\beta^{n,j}[U] := U^{n,j-1} + \beta \delta_\tau U^{n,j}$ and $\mathcal{Q}_{\beta,\gamma}^{n,j}[U] := U^{n,j-1} + \beta \delta_\tau U^{n,j} + \gamma(\tilde{U}^{n,j-1} + \beta \delta_\tau \tilde{U}^{n,j})$.

4.2 Stage regularity of time-discrete solutions

To establish the regularity of time stage solutions $U^{n,i}$ to the time-discrete system (4.6), we impose the following rough assumption

$$\|\zeta_{\mathbb{R}}^{n,i+1}\|_{L^2} \leq K_1 \tau_n \quad \text{for } 1 \leq n \leq N \text{ and } 1 \leq i \leq s_{\mathbb{I}}. \quad (4.11)$$

This setting (4.11) is imposed according to two facts: (1) assuming $\zeta_{\mathbb{R}}^{n,i+1} = 0$ for $1 \leq i \leq s_{\mathbb{I}} - 1$ would be not reasonable to derive the errors of stage solutions; (2) the first-order setting is to make the present analysis extendable to the Radau-type IERK methods in [8, 26].

4.2.1 H_{per}^2 norm boundedness of stage solutions

We will use the complete mathematical induction to prove that the stage solutions $U^{n,i}$ of the time-discrete system (4.6) are bounded in the H_{per}^2 norm, that is,

$$\|\tilde{U}^{n,i}\|_{H^2} \leq K_{10}/\epsilon^2 \quad \text{for } 1 \leq n \leq N \text{ and } 1 \leq i \leq s. \quad (4.12)$$

Obviously, it holds for $n = 1$ and $i = 1$ since $U^{1,1} = \Phi^0$. Put the inductive hypothesis

$$\|\tilde{U}^{l,\ell}\|_{H^2} \leq \kappa_{10}/\epsilon^2 \quad \text{such that} \quad \|U^{l,\ell}\|_{L^\infty} \leq \kappa_{10}^*/\epsilon^2 \quad \text{for } 1 \leq l \leq n \text{ and } 1 \leq \ell \leq k, \quad (4.13)$$

where $\kappa_{10}^* = K_\phi \epsilon^2 + K_\Omega K_{10}$. Now we are to prove that $\|\tilde{U}^{n,k+1}\|_{H^2} \leq \kappa_{10}/\epsilon^2$.

(L^2 norm rough estimate) Making the L^2 inner product of (4.9) by $2\tilde{U}^{n,i+\frac{1}{2}}$, applying the discrete Green's formula and summing the stage index i from $i = 1$ to k , one can find that

$$\begin{aligned} \|\tilde{U}^{n,k+1}\|_{L^2}^2 - \|\tilde{U}^{n,1}\|_{L^2}^2 &= 2\tau_n \sum_{i=1}^k \sum_{j=1}^i \hat{a}_{i+1,j} (L_\kappa \tilde{U}^{n,j+\frac{1}{2}}, \Delta \tilde{U}^{n,i+\frac{1}{2}})_{L^2} + 2\tau_n \sum_{i=1}^k (\delta_\tau \zeta_{\mathbb{R}}^{n,i+1}, \tilde{U}^{n,i+\frac{1}{2}})_{L^2} \\ &\quad + 2\tau_n \sum_{i=1}^k \sum_{j=1}^i \hat{a}_{i+1,j} (f_\kappa(U^{n,j}) - f_\kappa(\Phi^{n,j}), \Delta \tilde{U}^{n,i+\frac{1}{2}})_{L^2}. \end{aligned} \quad (4.14)$$

Lemma 4.3 (i) yields

$$2\tau_n \sum_{i=1}^k \sum_{j=1}^i \hat{a}_{i+1,j} (L_\kappa \tilde{U}^{n,j+\frac{1}{2}}, \Delta \tilde{U}^{n,i+\frac{1}{2}})_{L^2} \leq -2\epsilon^2 \sigma_{\min} \tau_n \sum_{i=1}^k \|\Delta \tilde{U}^{n,i+\frac{1}{2}}\|_{L^2}^2.$$

For the last term in (4.14), one can apply Lemma 4.3 (ii) and Lemma 4.4 (i) to derive that

$$\begin{aligned} 2\tau_n \sum_{i=1}^k \sum_{j=1}^i \hat{a}_{i+1,j} (f_\kappa(U^{n,j}) - f_\kappa(\Phi^{n,j}), \Delta \tilde{U}^{n,i+\frac{1}{2}})_{L^2} &\leq \frac{2\tau_n}{\lambda_{\min}} \sum_{i=1}^k \|f_\kappa(U^{n,i}) - f_\kappa(\Phi^{n,i})\|_{L^2} \|\Delta \tilde{U}^{n,i+\frac{1}{2}}\|_{L^2} \\ &\leq 2\epsilon^2 \sigma_{\min} \tau_n \sum_{i=1}^k \|\Delta \tilde{U}^{n,i+\frac{1}{2}}\|_{L^2}^2 + \frac{\tau_n}{2\lambda_{\min}^2 \sigma_{\min} \epsilon^2} \sum_{i=1}^k \|\tilde{U}^{n,i}\|_{L^2}^2 \int_0^1 (\kappa + \|F''(\mathbb{Q}_\gamma^{n,i}[U])\|_{L^\infty})^2 d\gamma, \end{aligned}$$

where $\mathbb{Q}_\gamma^{n,i}[U]$ is defined in Lemma 4.4 and then $\|F''(\mathbb{Q}_\gamma^{n,i}[U])\|_{L^\infty} \leq K_2 := \max_{\|\xi\|_{L^\infty} \leq \kappa_{10}^*/\epsilon^2} \|F''(\xi)\|_{L^\infty}$

according to the uniform bound (4.13). Thus, it follows from (4.14) that

$$\|\tilde{U}^{n,k+1}\|_{L^2}^2 - \|\tilde{U}^{n,1}\|_{L^2}^2 \leq \frac{K_3 \tau_n}{\epsilon^2} \sum_{i=1}^k \|\tilde{U}^{n,i}\|_{L^2}^2 + 2\tau_n \sum_{i=1}^k \|\delta_\tau \zeta_{\mathbb{R}}^{n,i+1}\|_{L^2} \|\tilde{U}^{n,i+1}\|_{L^2}, \quad (4.15)$$

where the constant $K_3 := \frac{(K_2 + \kappa)^2}{2\sigma_{\min} \lambda_{\min}^2}$. For any index n , choose a finite k_0 satisfying $1 \leq k_0 \leq k$ such that $\|\tilde{U}^{n,k_0+1}\|_{L^2} := \max_{0 \leq \ell \leq k} \|\tilde{U}^{n,\ell+1}\|_{L^2}$. We set $k = k_0$ in (4.15) to get

$$\|\tilde{U}^{n,k_0+1}\|_{L^2} \leq \|\tilde{U}^{n,1}\|_{L^2} + \frac{K_3 \tau_n}{\epsilon^2} \sum_{i=1}^{k_0} \|\tilde{U}^{n,i}\|_{L^2} + 2\tau_n \sum_{i=1}^{k_0} \|\delta_\tau \zeta_{\mathbb{R}}^{n,i+1}\|_{L^2},$$

and then, due to $k_0 \leq k$ and $\|\tilde{U}^{n,k+1}\|_{L^2} \leq \|\tilde{U}^{n,k_0+1}\|_{L^2}$,

$$\|\tilde{U}^{n,k+1}\|_{L^2} \leq \|\tilde{U}^{n,1}\|_{L^2} + \frac{K_3 \tau_n}{\epsilon^2} \sum_{i=1}^k \|\tilde{U}^{n,i}\|_{L^2} + 2\tau_n \sum_{i=1}^k \|\delta_\tau \zeta_{\mathbb{R}}^{n,i+1}\|_{L^2}. \quad (4.16)$$

By using the defect bound (4.11), the discrete Grönwall inequality in Lemma 4.2 together with the maximum time-step condition $\tau \leq \epsilon^2/K_3$ gives

$$\|\tilde{U}^{n,k+1}\|_{L^2} \leq 4^s \exp(2^{s-1} K_3 t_{n-1}/\epsilon^2) s_1 K_1 t_n \tau \leq K_4 \tau, \quad (4.17)$$

where the constant $K_4 := 4^s \exp(2^{s-1} K_3 T/\epsilon^2) s_1 K_1 T$.

(H_{per}^2 seminorm rough estimate) Making the L^2 inner product of (4.10) by $\frac{2}{\epsilon^2}\delta_\tau\tilde{U}^{n,j+1}$, applying the discrete Green's formula and summing j from $j = 1$ to k , one can find that

$$\begin{aligned} \|\Delta\tilde{U}^{n,k+1}\|_{L^2}^2 - \|\Delta\tilde{U}^{n,1}\|_{L^2}^2 &= -\frac{2}{\epsilon^2\tau_n} \sum_{j=1}^k \sum_{i=1}^j d_{j,i}^{(R)}(\delta_\tau\tilde{U}^{n,i+1}, \delta_\tau\tilde{U}^{n,j+1})_{L^2} - \frac{\kappa}{\epsilon^2} \sum_{j=1}^k \|\delta_\tau\nabla\tilde{U}_h^{n,j+1}\|_{L^2}^2 \\ &+ \frac{2}{\epsilon^2} \sum_{j=1}^k (F'(U^{n,j}) - F'(\Phi^{n,j}), \delta_\tau\Delta\tilde{U}^{n,j+1})_{L^2} + \frac{2}{\epsilon^2} \sum_{j=1}^k \sum_{i=1}^j d_{j,i}^{(R)}(\delta_\tau\zeta_R^{n,i+1}, \delta_\tau\tilde{U}^{n,j+1})_{L^2}. \end{aligned} \quad (4.18)$$

According to Lemma 4.3 (i), one has

$$-\frac{2}{\epsilon^2\tau_n} \sum_{j=1}^k \sum_{i=1}^j d_{j,i}^{(R)}(\delta_\tau\tilde{U}^{n,i+1}, \delta_\tau\tilde{U}^{n,j+1})_{L^2} \leq -\frac{2\lambda_{\min}}{\epsilon^2\tau_n} \sum_{j=1}^k \|\delta_\tau\tilde{U}^{n,j+1}\|_{L^2}^2.$$

With the help of Lemma 4.3 (ii) and the Young inequality, one gets

$$\begin{aligned} \frac{2}{\epsilon^2} \sum_{j=1}^k \sum_{i=1}^j d_{j,i}^{(R)}(\delta_\tau\zeta_R^{n,i+1}, \delta_\tau\tilde{U}^{n,j+1})_{L^2} &\leq \frac{2}{\sigma_{\min}\epsilon^2} \sum_{j=1}^k \|\delta_\tau\zeta_R^{n,j+1}\|_{L^2} \|\delta_\tau\tilde{U}^{n,j+1}\|_{L^2} \\ &\leq \frac{\lambda_{\min}}{\epsilon^2\tau_n} \sum_{j=1}^k \|\delta_\tau\tilde{U}^{n,j+1}\|_{L^2}^2 + \frac{\tau_n}{\lambda_{\min}\sigma_{\min}^2\epsilon^2} \sum_{j=1}^k \|\delta_\tau\zeta_R^{n,j+1}\|_{L^2}^2. \end{aligned}$$

To bound the nonlinear term, we recall the Abel-type formula of summation-by-part, also see [20, 21], $\sum_{j=1}^k u^j(v^{j+1} - v^j) = u^k v^{k+1} - \sum_{j=2}^k v^j(u^j - u^{j-1}) - u^1 v^1$. One applies Lemma 4.4 to get

$$\begin{aligned} J_k &:= \frac{2}{\epsilon^2} \sum_{j=1}^k (F'(U^{n,j}) - F'(\Phi^{n,j}), \delta_\tau\Delta\tilde{U}^{n,j+1})_{L^2} = \frac{2}{\epsilon^2} (F'(U^{n,k}) - F'(\Phi^{n,k}), \Delta\tilde{U}^{n,k+1})_{L^2} \\ &+ \frac{2}{\epsilon^2} (F'(U^{n,1}) - F'(\Phi^{n,1}), \Delta\tilde{U}^{n,1})_{L^2} - \frac{2}{\epsilon^2} \sum_{j=2}^k (\delta_\tau F'(U^{n,j}) - \delta_\tau F'(\Phi^{n,j}), \Delta\tilde{U}^{n,j})_{L^2} \triangleq \sum_{\ell=1}^3 J_{k,\ell}, \end{aligned}$$

where, by using the discrete functionals $\mathcal{Q}_\gamma^{n,j}[U]$, $\mathcal{Q}_\beta^{n,j}[U]$ and $\mathcal{Q}_{\beta,\gamma}^{n,j}[U]$ defined in Lemma 4.4,

$$\begin{aligned} J_{k,1} &\leq \frac{2}{\epsilon^2} \|\tilde{U}^{n,k}\|_{L^2} \|\Delta\tilde{U}^{n,k+1}\|_{L^2} \int_0^1 \|F''(\mathcal{Q}_\gamma^{n,k}[U])\|_{L^\infty} d\gamma, \\ J_{k,2} &\leq \frac{2}{\epsilon^2} \|\tilde{U}^{n,1}\|_{L^2} \|\Delta\tilde{U}^{n,1}\|_{L^2} \int_0^1 \|F''(\mathcal{Q}_\gamma^{n,1}[U])\|_{L^\infty} d\gamma, \\ J_{k,3} &\leq \frac{4K_\phi\tau_n}{\epsilon^2} \sum_{j=2}^k \|\Delta\tilde{U}^{n,j}\|_{L^2} (\|\tilde{U}^{n,j}\|_{L^2} + \|\tilde{U}^{n,j-1}\|_{L^2}) \int_0^1 \int_0^1 \|F'''(\mathcal{Q}_{\beta,\gamma}^{n,j}[U])\|_{L^\infty} d\gamma d\beta \\ &+ \frac{2}{\epsilon^2} \sum_{j=2}^k \|\Delta\tilde{U}^{n,j}\|_{L^2} \|\delta_\tau\tilde{U}^{n,j}\|_{L^2} \int_0^1 \|F''(\mathcal{Q}_\beta^{n,j}[U])\|_{L^\infty} d\beta \\ &\leq \frac{4K_\phi\tau_n}{\epsilon^2} \sum_{j=2}^k \|\Delta\tilde{U}^{n,j}\|_{L^2} (\|\tilde{U}^{n,j}\|_{L^2} + \|\tilde{U}^{n,j-1}\|_{L^2}) \int_0^1 \int_0^1 \|F'''(\mathcal{Q}_{\beta,\gamma}^{n,j}[U])\|_{L^\infty} d\gamma d\beta \\ &+ \frac{\tau_n}{\lambda_{\min}\epsilon^2} \sum_{j=2}^k \|\Delta\tilde{U}^{n,j}\|_{L^2}^2 \int_0^1 \|F''(\mathcal{Q}_\beta^{n,j}[U])\|_{L^\infty}^2 d\beta + \frac{\lambda_{\min}}{\epsilon^2\tau_n} \sum_{j=1}^k \|\delta_\tau\tilde{U}^{n,j+1}\|_{L^2}^2. \end{aligned}$$

Applying the maximum norm bound (4.13) of stage solutions, one has $\|F''(\mathbf{Q}_\gamma^{n,i}[U])\|_{L^\infty} \leq K_2$,

$$\|F''(\mathbf{Q}_\beta^{n,i}[U])\|_{L^\infty} \leq K_2 \quad \text{and} \quad \|F'''(\mathbf{Q}_{\beta,\gamma}^{n,i}[U])\|_{L^\infty} \leq K_5 := \max_{\|\xi\|_{L^\infty} \leq 2K_{10}^*/\epsilon^2} \|F'''(\xi)\|_{L^\infty}.$$

By collecting the above estimates, it follows from (4.18) that

$$\begin{aligned} \|\Delta \tilde{U}^{n,k+1}\|_{L^2}^2 &\leq \|\Delta \tilde{U}^{n,1}\|_{L^2}^2 + \frac{2K_2}{\epsilon^2} \|\tilde{U}^{n,k}\|_{L^2} \|\Delta \tilde{U}^{n,k+1}\|_{L^2} + \frac{2K_2}{\epsilon^2} \|\tilde{U}^{n,1}\|_{L^2} \|\Delta \tilde{U}^{n,1}\|_{L^2} \\ &\quad + \frac{4K_5 K_\phi \tau_n}{\epsilon^2} \sum_{j=2}^k \|\Delta \tilde{U}^{n,j}\|_{L^2} (\|\tilde{U}^{n,j}\|_{L^2} + \|\tilde{U}^{n,j-1}\|_{L^2}) \\ &\quad + \frac{K_6 \tau_n}{\epsilon^2} \sum_{j=2}^k \|\Delta \tilde{U}^{n,j}\|_{L^2}^2 + \frac{\tau_n}{\lambda_{\min} \sigma_{\min}^2 \epsilon^2} \sum_{j=1}^k \|\delta_\tau \zeta_{\mathbf{R}}^{n,j+1}\|_{L^2}^2, \end{aligned} \quad (4.19)$$

where the constant $K_6 := \frac{K_2^2}{\lambda_{\min}}$. It is reasonable to assume further that the maximum time-step size is small such that $N\tau \leq K_T T$. Also, let the constants $K_7 := 2^{2s-1} \exp(2^{s-1} K_6 T/\epsilon^2) \frac{\sqrt{T} s_1 K_1}{\sigma_{\min} \sqrt{\lambda_{\min}}}$, $K_8 := 2^{2s+1} \exp(2^{s-1} K_6 T/\epsilon^2) K_4 K_5 K_\phi T s_1$ and $K_9 := 4^s \exp(2^{s-1} K_6 T/\epsilon^2) K_2 K_4 K_T T$. One can claim from the inequality (4.19) that

$$\|\Delta \tilde{U}^{n,k+1}\|_{L^2} \leq (K_7 \epsilon + K_8) \tau / \epsilon^2 + K_9 / \epsilon^2 \quad \text{if } \tau \leq \epsilon^2 / K_6. \quad (4.20)$$

For any fixed n , two different cases are considered: (Case H2-1) if the H_{per}^2 semi-norm

$$\|\Delta \tilde{U}^{n,j+1}\|_{L^2} \leq \frac{\sqrt{T}}{\sigma_{\min} \sqrt{\lambda_{\min}} \epsilon} \max_{1 \leq j \leq s_1} \|\delta_\tau \zeta_{\mathbf{R}}^{n,j+1}\|_{L^2} \quad \text{for } 1 \leq j \leq k,$$

the H_{per}^2 semi-norm bound (4.20) follows immediately. (Case H2-2) Otherwise, one can set

$$\frac{\sigma_{\min} \sqrt{\lambda_{\min}} \epsilon}{\sqrt{T}} \|\Delta \tilde{U}^{n,j+1}\|_{L^2} \geq \max_{1 \leq j \leq s_1} \|\delta_\tau \zeta_{\mathbf{R}}^{n,j+1}\|_{L^2} \geq \|\delta_\tau \zeta_{\mathbf{R}}^{n,j+1}\|_{L^2} \quad \text{for } 1 \leq j \leq k,$$

such that the inequality (4.19) can be reduced into, cf. the derivations from (4.15) to (4.16),

$$\begin{aligned} \|\Delta \tilde{U}^{n,k+1}\|_{L^2} &\leq \|\Delta \tilde{U}^{n,1}\|_{L^2} + \frac{K_6 \tau_n}{\epsilon^2} \sum_{j=2}^k \|\Delta \tilde{U}^{n,j}\|_{L^2} + \frac{\tau_n}{\sigma_{\min} \sqrt{\lambda_{\min}} T \epsilon} \sum_{j=1}^k \|\delta_\tau \zeta_{\mathbf{R}}^{n,j+1}\|_{L^2} \\ &\quad + \frac{4K_2}{\epsilon^2} \max_{1 \leq j \leq k} \|\tilde{U}^{n,j}\|_{L^2} + \frac{4K_5 K_\phi \tau_n}{\epsilon^2} \sum_{j=2}^k (\|\tilde{U}^{n,j}\|_{L^2} + \|\tilde{U}^{n,j-1}\|_{L^2}). \end{aligned}$$

By using the defect bound (4.11) and the L^2 norm estimate (4.17), the discrete Grönwall inequality in Lemma 4.2 together with the maximum time-step condition $\tau \leq \epsilon^2 / K_6$ gives

$$\begin{aligned} \|\Delta \tilde{U}^{n,k+1}\|_{L^2} &\leq 4^{s-1} \exp(2^{s-1} K_6 T/\epsilon^2) \left(\frac{2\sqrt{T} s_1 K_1 \epsilon}{\sigma_{\min} \sqrt{\lambda_{\min}}} \tau + 8K_4 K_5 K_\phi T s_1 \tau + 4K_2 K_4 n \tau \right) / \epsilon^2 \\ &\leq (K_7 \epsilon + K_8) \tau / \epsilon^2 + K_9 / \epsilon^2. \end{aligned}$$

The above two cases (Case H2-1) and (Case H2-2) verify the H_{per}^2 semi-norm bound (4.20).

By combining (4.17) with (4.20), one can get the desired H_{per}^2 norm bound $\|\tilde{U}^{n,k+1}\|_{H^2} \leq K_{10} / \epsilon^2$ by taking $K_{10} := K_4 \epsilon^2 / K_3 + (K_7 \epsilon + K_8) \epsilon^2 / K_6 + K_9$. That is, the estimate (4.13) holds for $l = n$ and $\ell = k + 1$ and the mathematical induction arrives at the H_{per}^2 norm bound (4.12).

4.2.2 H_{per}^{m+4} norm boundedness of stage solutions

It is to note that, the above proof of the H_{per}^2 norm bound (4.12) can be extended to derive the following H_{per}^3 norm bound of stage solutions via the mathematical induction,

$$\|\tilde{U}^{n,i}\|_{H^3} \leq K_{16}/\epsilon^2 \quad \text{for } 1 \leq n \leq N \text{ and } 1 \leq i \leq s.$$

Under the inductive hypothesis with $K_{16}^* := K_\phi \epsilon^2 + K_\Omega K_{16}$,

$$\|\tilde{U}^{l,\ell}\|_{H^3} \leq K_{16}/\epsilon^2 \quad \text{such that} \quad \|\nabla U^{l,\ell}\|_{L^\infty} \leq K_{16}^*/\epsilon^2 \quad \text{for } 1 \leq l \leq n \text{ and } 1 \leq \ell \leq k,$$

one can follow the proof of Lemma 4.4 to establish similar bounds for $\|\nabla F'(\Phi^{n,j}) - \nabla F'(U^{n,j})\|_{L^2}$ and $\|\delta_\tau \nabla F'(\Phi^{n,j}) - \delta_\tau \nabla F'(U^{n,j})\|_{L^2}$. With these bounds of nonlinear term and the discrete Grönwall inequality in Lemma 4.2, one can derive the H^1 semi-norm error bound $\|\nabla \tilde{U}^{n,k+1}\|_{L^2} \leq K_{12}\tau$ (under the maximum time-step size $\tau \leq \epsilon^2/K_{11}$) by making the inner product of (4.9) by $2\Delta \tilde{U}^{n,i+\frac{1}{2}}$ and following the derivations in (**L^2 norm rough estimate**). After that, we can make the inner product of (4.10) by $\frac{2}{\epsilon^2} \delta_\tau \Delta \tilde{U}^{n,j+1}$ and follow the derivations of (**H^2 seminorm rough estimate**) to get H_{per}^3 semi-norm error bound $\|\nabla \Delta \tilde{U}^{n,k+1}\|_{L^2} \leq K_{14}\tau/\epsilon^2 + K_{15}/\epsilon^2$ (under the maximum time-step size $\tau \leq \epsilon^2/K_{13}$ and $\tau \leq K_T T/N$). Then we can complete the mathematical induction by taking the constant $K_{16} := K_{12}\epsilon^2/K_{11} + K_{14}\epsilon^2/K_{13} + K_{15}$.

By performing the above process repeatedly, one can check that there exists a positive constant K_ϕ , independent of τ_n , such that the stage solutions $U^{n,i}$ fulfill $\|U^{n,i}\|_{H^{m+4}} \leq K_\phi/\epsilon^2$ for $1 \leq n \leq N$ and $2 \leq i \leq s$. Combining it with the time-discrete system (4.6), we have the following theorem.

Theorem 4.1. *Assume that the solution of the CH problem (1.2) satisfies the regularity assumption (4.5) with $m \geq 1$, and the differentiation matrix $D_R = A_E^{-1} E_{s_1}$ of the R-IERK method (2.10) and the inverse D_R^{-1} are positive definite. If the maximum time-step size τ is sufficiently small, there exists a positive constant K_ϕ , independent of the time-step sizes τ_n , such that the stage solutions $U^{n,i}$ of the time-discrete system (4.6) are bounded,*

$$\|U^{n,i}\|_{H^{m+4}} + \|(U^{n,i} - U^{n,1})/\tau_n\|_{H^m} \leq K_\phi/\epsilon^2 \quad \text{for } 1 \leq n \leq N \text{ and } 2 \leq i \leq s.$$

4.3 Uniform boundedness of stage solutions and discrete energy law

4.3.1 Fully discrete error system

As seen from Lemma 2.1, proving the uniform boundedness of stage solutions $u_h^{n,i}$ is necessary to establish the energy dissipation laws for the fully-discrete R-IERK method (2.10), which can be viewed as the spatial approximation of the time discrete system (4.7).

In general, we evaluate the stage error by a usual splitting, $U^{n,\ell} - u_h^{n,\ell} = U^{n,\ell} - U_M^{n,\ell} + e_h^{n,\ell}$, where $U_M^{n,\ell} := P_M U^{n,\ell}$ is the L^2 projection of time-discrete solution $U^{n,\ell}$ and $e_h^{n,\ell} := U_M^{n,\ell} - u_h^{n,\ell} \in \mathring{V}_h$ is the difference between the projection $U_M^{n,\ell}$ and the solution $u_h^{n,\ell}$ of the R-IERK method (2.10). Without losing the generality, we set the initial data $u_h^{1,1} := U_M^{1,1}$ such that $e_h^{1,1} = 0$. Note that, the L^2 projection solution $U_M^{n,\ell} \in \mathcal{F}_M$ and the volume conservation (2.4) arrive at

$$\langle U_M^{n,\ell}, 1 \rangle = \langle U_M^{1,1}, 1 \rangle = \langle u^{1,1}, 1 \rangle = \langle u^{n,\ell}, 1 \rangle,$$

so that the error function $e^{n,\ell} \in \mathring{V}_h$. Applying Lemma 4.1 with $U^{n,\ell} \in C^2([0, T]; H_{per}^m)$, one has

$$\|U^{n,\ell} - U_M^{n,\ell}\| = \|I_M(U^{n,\ell} - U_M^{n,\ell})\|_{L^2} \leq K_\phi \|I_M U^{n,\ell} - U_M^{n,\ell}\|_{L^2} \leq K_\phi h^m |U^{n,\ell}|_{H^m}.$$

Once the upper bound of $\|e^n\|$ is available, the L^2 norm error estimate follows immediately,

$$\|U^{n,\ell} - u^{n,\ell}\| \leq \kappa_\phi h^m / \epsilon^2 + \|e^{n,\ell}\| \quad \text{for } 1 \leq n \leq N \text{ and } 1 \leq \ell \leq s_I. \quad (4.21)$$

To bound the L^2 norm of $e_h^{n,\ell}$, we consider the space consistency error for a semi-discrete system having a projected solution U_M . A substitution of the L^2 projection solution U_M and differentiation operator Δ_h into the equation (4.6) yields the discrete system

$$U_M^{n,i+1} = U_M^{n,1} + \tau_n \sum_{j=1}^i \hat{a}_{i+1,j} \Delta_h \left[L_{\kappa,h} U_M^{n,j+\frac{1}{2}} - f_\kappa(U_M^{n,j}) \right] + \tau_n \zeta_P^{n,i+1} \quad (4.22)$$

for $n \geq 1$ and $1 \leq i \leq s_I$, where $\zeta_P^{n,i+1} = \zeta_P(\mathbf{x}_h, t_{n,i+1})$ represents the spatial consistency error arising from the L^2 projection of time-discrete solution $U^{n,j}$, that is,

$$\begin{aligned} \zeta_P^{n,i+1} := & \frac{1}{\tau_n} (U_M^{n,i+1} - U_M^{n,1}) - \sum_{j=1}^i \hat{a}_{i+1,j} \Delta_h \left[L_{\kappa,h} U_M^{n,j+\frac{1}{2}} - f_\kappa(U_M^{n,j}) \right] \\ & - \frac{1}{\tau_n} (U^{n,i+1} - U^{n,1}) + \sum_{j=1}^i \hat{a}_{i+1,j} \Delta \left[L_\kappa U^{n,j+\frac{1}{2}} - f_\kappa(U^{n,j}) \right] \quad \text{for } \mathbf{x}_h \in \Omega_h. \end{aligned}$$

By Theorem 4.1 and Lemma 4.1, one can follow the proof of [22, Theorem 3.1] to obtain

$$\|\zeta_P^{n,i+1}\| \leq \kappa_\phi h^m \max_{1 \leq i \leq s_I} (\|U^{n,i+1}\|_{H^{m+4}} + \frac{1}{\tau_n} \|U^{n,i+1} - U^{n,1}\|_{H^m}) \leq \hat{\kappa}_1 h^m / \epsilon^2. \quad (4.23)$$

Subtracting the fully discrete scheme (2.10) from (4.22), one has the following error system

$$e_h^{n,i+1} = e_h^{n,1} + \tau_n \sum_{j=1}^i \hat{a}_{i+1,j} \Delta_h \left[L_{\kappa,h} e_h^{n,j+\frac{1}{2}} + f_\kappa(u_h^{n,j}) - f_\kappa(U_M^{n,j}) \right] + \tau_n \zeta_P^{n,i+1}$$

or, with the matrix $(\hat{a}_{i+1,j})_{s_I \times s_I} = E_{s_I}^{-1} A_E = D_R^{-1}$,

$$\delta_\tau e_h^{n,i+1} = \tau_n \sum_{j=1}^i \hat{a}_{i+1,j} \Delta_h \left[L_{\kappa,h} e_h^{n,j+\frac{1}{2}} + f_\kappa(u_h^{n,j}) - f_\kappa(U_M^{n,j}) \right] + \tau_n \delta_\tau \zeta_P^{n,i+1} \quad (4.24)$$

for $n \geq 1$ and $1 \leq i \leq s_I$.

4.3.2 Uniform boundedness of fully discrete solutions

We use the complete mathematical induction to prove that the stage solutions $u_h^{n,i}$ of the fully discrete scheme (2.10) are bounded in the L^2 norm, that is,

$$\|e^{n,i}\| \leq \hat{\kappa}_4 h^m / \epsilon^2 \quad \text{for } 1 \leq n \leq N \text{ and } 1 \leq i \leq s. \quad (4.25)$$

Obviously, it holds for $n = 1$ and $i = 1$ since $e^{1,1} = 0$. Put the inductive hypothesis

$$\|e^{l,\ell}\| \leq \hat{\kappa}_4 h^m / \epsilon^2 \quad \text{for } 1 \leq l \leq n \text{ and } 1 \leq \ell \leq k, \quad (4.26)$$

such that $\|e^{l,\ell}\|_\infty \leq h^{-1} \|e^{l,\ell}\| \leq \hat{\kappa}_4 h^{m-1} / \epsilon^2 \leq 1$ if $h \leq \frac{m-1}{\sqrt{\epsilon^2 / \hat{\kappa}_4}}$ and thus

$$\|u^{l,\ell}\|_\infty \leq \|U_M^{l,\ell}\|_\infty + \|e^{l,\ell}\|_\infty \leq \hat{\kappa}_4^* / \epsilon^2 \quad \text{for } 1 \leq l \leq n \text{ and } 1 \leq \ell \leq k, \quad (4.27)$$

where the constant $\hat{K}_4^* := \kappa_\phi + \epsilon^2$. In the following, we are to prove that $\|e^{n,k+1}\| \leq \hat{K}_4 h^m / \epsilon^2$.

Making the inner product of (4.24) by $2e_h^{n,i+\frac{1}{2}}$, applying the discrete Green's formula and summing the stage index i from $i = 1$ to k , one can find that

$$\begin{aligned} \|e^{n,k+1}\|^2 - \|e^{n,1}\|^2 &= 2\tau_n \sum_{i=1}^k \sum_{j=1}^i \hat{a}_{i+1,j} \langle L_{\kappa,h} e^{n,j+\frac{1}{2}}, \Delta_h e^{n,i+\frac{1}{2}} \rangle + 2\tau_n \sum_{i=1}^k \langle \delta_\tau \zeta_P^{n,i+1}, e^{n,i+\frac{1}{2}} \rangle \\ &\quad + 2\tau_n \sum_{i=1}^k \sum_{j=1}^i \hat{a}_{i+1,j} \langle f_\kappa(u^{n,j}) - f_\kappa(U_M^{n,j}), \Delta_h e^{n,i+\frac{1}{2}} \rangle. \end{aligned} \quad (4.28)$$

Lemma 4.3 (i) yields

$$2\tau_n \sum_{i=1}^k \sum_{j=1}^i \hat{a}_{i+1,j} \langle L_{\kappa,h} e^{n,j+\frac{1}{2}}, \Delta_h e^{n,i+\frac{1}{2}} \rangle \leq -2\epsilon^2 \sigma_{\min} \tau_n \sum_{i=1}^k \|\Delta_h e^{n,i+\frac{1}{2}}\|^2.$$

For the last term in (4.28), one can apply Lemma 4.3 (ii) and Lemma 4.4 (i) to derive that

$$\begin{aligned} 2\tau_n \sum_{i=1}^k \sum_{j=1}^i \hat{a}_{i+1,j} \langle f_\kappa(u^{n,j}) - f_\kappa(U_M^{n,j}), \Delta_h e^{n,i+\frac{1}{2}} \rangle &\leq \frac{2\tau_n}{\lambda_{\min}} \sum_{i=1}^k \|f_\kappa(u^{n,i}) - f_\kappa(U_M^{n,i})\| \|\Delta_h e^{n,i+\frac{1}{2}}\| \\ &\leq 2\epsilon^2 \sigma_{\min} \tau_n \sum_{i=1}^k \|\Delta_h e^{n,i+\frac{1}{2}}\|^2 + \frac{\tau_n}{2\sigma_{\min} \lambda_{\min}^2 \epsilon^2} \sum_{i=1}^k \|e^{n,i}\|^2 \int_0^1 (\kappa + \|F''(Q_{\gamma,h}^{n,i}[u])\|_\infty)^2 d\gamma, \end{aligned}$$

where the discrete functional $Q_{\gamma,h}^{n,i}[u]$ is defined via Lemma 4.4, that is, $Q_{\gamma,h}^{n,j}[u] := U_M^{n,j} + \gamma e_h^{n,j}$, so that $\|F''(Q_{\gamma,h}^{n,i}[u])\|_\infty \leq \hat{K}_2 := \max_{\|\xi\|_\infty \leq \hat{K}_4^* / \epsilon^2} \|F''(\xi)\|_\infty$ according to the maximum norm bound (4.27). Thus, it follows from (4.28) that

$$\|e^{n,k+1}\|^2 - \|e^{n,1}\|^2 \leq \frac{\hat{K}_3 \tau_n}{\epsilon^2} \sum_{i=1}^k \|e^{n,i}\|^2 + 2\tau_n \sum_{i=1}^{\ell} \|\delta_\tau \zeta_P^{n,i+1}\| \|e^{n,i+1}\|, \quad (4.29)$$

where the constant $\hat{K}_3 := \frac{(\hat{K}_2 + \kappa)^2}{2\sigma_{\min} \lambda_{\min}^2}$. For any index n , choose k_0 satisfying $1 \leq k_0 \leq k$ such that $\|e^{n,k_0+1}\| := \max_{0 \leq \ell \leq k} \|e^{n,\ell+1}\|$. We set $k = k_0$ in (4.29) to get

$$\|e^{n,k_0+1}\| \leq \|e^{n,1}\| + \frac{\hat{K}_3 \tau_n}{\epsilon^2} \sum_{i=1}^{k_0} \|e^{n,i}\| + 2\tau_n \sum_{i=1}^{k_0} \|\delta_\tau \zeta_P^{n,i+1}\|,$$

and then, due to $k_0 \leq k$ and $\|e^{n,k+1}\| \leq \|e^{n,k_0+1}\|$,

$$\|e^{n,k+1}\| \leq \|e^{n,1}\| + \frac{\hat{K}_3 \tau_n}{\epsilon^2} \sum_{i=1}^k \|e^{n,i}\| + 2\tau_n \sum_{i=1}^k \|\delta_\tau \zeta_P^{n,i+1}\|.$$

By using the truncation error bound (4.23), the discrete Grönwall inequality in Lemma 4.2 together with the maximum time-step condition $\tau \leq \epsilon^2 / \hat{K}_3$ gives

$$\|e^{n,k+1}\| \leq 4^s \exp(2^{s-1} \hat{K}_3 t_{n-1} / \epsilon^2) s_1 \hat{K}_1 t_n h^m / \epsilon^2 \leq \hat{K}_4 h^m / \epsilon^2,$$

where the constant $\hat{K}_4 := 4^s \exp(2^{s-1} \hat{K}_3 T / \epsilon^2) s_1 \hat{K}_1 T$.

It says that the estimate (4.26) holds for $l = n$ and $\ell = k + 1$. Thus the principle of mathematical induction confirms the L^2 norm error estimate (4.25). The inverse estimate yields

$$\|u^{n,i}\|_\infty \leq \hat{K}_4^*/\epsilon^2 \quad \text{for } 1 \leq n \leq N \text{ and } 1 \leq i \leq s \quad \text{if } h \leq \sqrt[m-1]{\epsilon^2/\hat{K}_4}. \quad (4.30)$$

Thanks to the maximum norm bound (4.30) of stage solutions, one can take the positive constant $\kappa_0 := \hat{K}_4^*/\epsilon^2$ in Lemma 2.1 to obtain the following result.

Theorem 4.2. *Assume that the solution of the CH problem (1.2) satisfies the regularity assumption (4.5) with $m \geq 1$, and the differentiation matrix $D_R = A_E^{-1} E_{s_1}$ of the R-IERK method (2.10) and the inverse D_R^{-1} are positive definite. If the spatial length h and the maximum step size τ are sufficiently small, and the parameter κ in (1.4) is chosen properly large such that $\kappa \geq \max_{\|\xi\|_\infty \leq \hat{K}_4^*/\epsilon^2} \|F''(\xi)\|_\infty$, then the stage solutions $u_h^{n,i}$ of the R-IERK method (2.10) are bounded in the maximum norm and they preserve the original energy dissipation law (1.3) at all stages,*

$$E[u^{n,j+1}] - E[u^{n,1}] \leq \frac{1}{\tau} \sum_{k=1}^j \left\langle \Delta_h^{-1} \delta_\tau u^{n,k+1}, \sum_{\ell=1}^k d_{k\ell}^{(R)} \delta_\tau u^{n,\ell+1} \right\rangle \quad \text{for } 1 \leq n \leq N \text{ and } 1 \leq j \leq s_1.$$

4.4 L^2 norm estimate with full accuracy

For the convergence of the R-IERK method (2.10), we will overlook the defects at internal stages as done in the literature, cf. [7, 8], and assume that the stage temporal defects $\zeta_R^{n,i+1}$ satisfy

$$\zeta_R^{n,i+1} = 0 \quad \text{for } 1 \leq i \leq s_1 \quad \text{and} \quad \|\zeta_R^{n,s}\| \leq \kappa_2 \tau^p \quad \text{for } 1 \leq n \leq N. \quad (4.31)$$

Actually, the rough setting (4.11) is not enough to derive the sharp error estimate at time levels with fully accuracy. With the help of Theorem 4.2, the following result can be verified by following the L^2 norm estimate in subsection 4.3. The technical details are left to interested readers.

Theorem 4.3. *Assume that the solution of the CH problem (1.2) satisfies the regularity assumption (4.5) with $m \geq 1$, and the differentiation matrix $D_R = A_E^{-1} E_{s_1}$ of the R-IERK method (2.10) and the inverse D_R^{-1} are positive definite. If the spatial length h and the maximum step size τ are sufficiently small, and the parameter κ in (1.4) is chosen properly such that $\kappa \geq \max_{\|\xi\|_\infty \leq \hat{K}_4^*/\epsilon^2} \|F''(\xi)\|_\infty$, then the solution u_h^n of R-IERK method (2.10) is convergent in the L^2 norm with an order of $\mathcal{O}(\tau^p + h^m)$.*

5 Numerical experiments

Example 2. *Consider the Cahn-Hilliard model (1.2) with an exterior force $g(x, y, t)$ subject to the initial data $\Phi^0 = \sin(\pi x) \sin(\pi y)$ on $\Omega = (0, 2)^2$ with the interface parameter $\epsilon = 0.2$. The source term g is set by choosing the exact solution $\Phi(x, y, t) = e^{-t} \sin(\pi x) \sin(\pi y)$. Always, the spatial operators are approximated by the Fourier pseudo-spectral approximation with 64×64 grid points.*

We examine the convergence of the R-IERK(2,4; c_2) method (3.2) and the R-IERK(3,6; \hat{a}_{52}) method (3.4) by choosing the final time $T = 1$ and the stabilized parameter $\kappa = 4$. Figure 2 lists the L^∞ norm error $e(\tau) := \max_{1 \leq n \leq N} \|\Phi_h^n - \Phi(t_n)\|_\infty$ for the two R-IERK methods on halving time steps $\tau = 2^{-k}/10$ for $0 \leq k \leq 9$. As expected, the R-IERK(2,4; c_2) method (3.2) and R-IERK(3,6; \hat{a}_{52}) method (3.4) are second-order and third-order accurate in time, respectively. It suggests that the different parameters for the R-IERK(2,4; c_2) method (3.2) would arrive at different precision and the case $c_2 = 1$ generates the most accurate solution when τ is smaller than 10^{-2} ; while the R-IERK(3,6; \hat{a}_{52}) method (3.4) with different parameters generates almost the same solution.

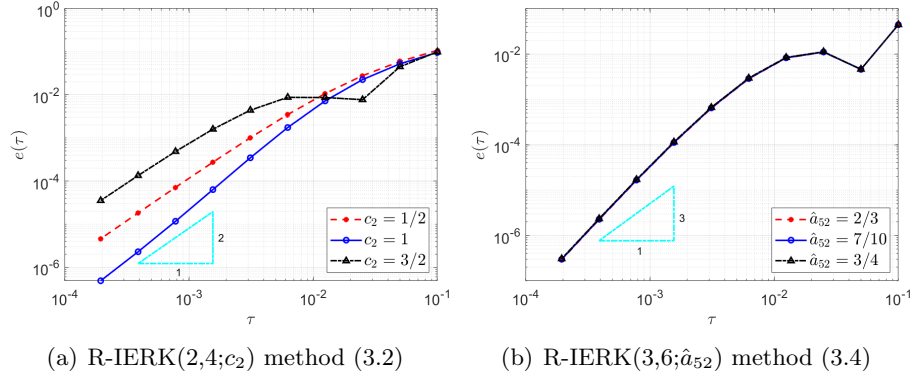


Figure 2: Solution errors of the two R-IERK methods with different parameters.

5.1 Tests of R-IERK(2,4; c_2) methods

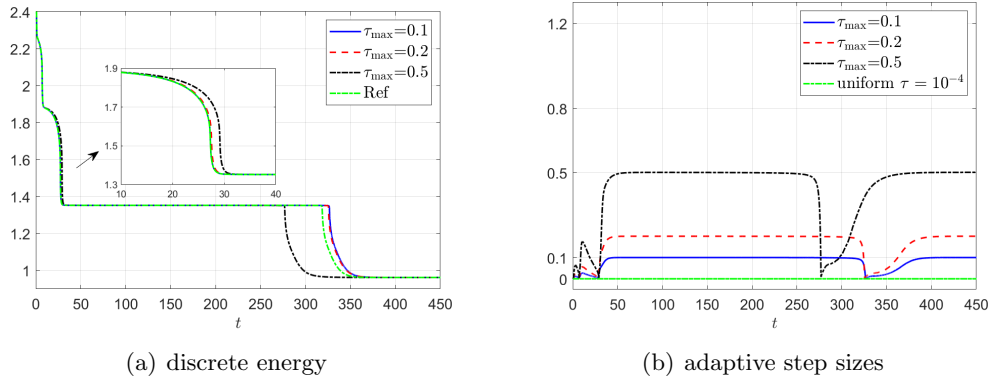


Figure 3: Energy curves and adaptive time-step sizes of R-IERK(2,4;1) method.

We examine the discrete energy behaviors by running the IERK(2,3) method and the R-IERK(2,4; c_2) method (3.2) with three different parameters $c_2 = \frac{1}{2}, 1$ and $\frac{3}{2}$ by the same adaptive time-stepping strategy adopted in Example 1. The reference solution is generated by the IERK(2,3) method with $\tau = 10^{-4}$, while in the adaptive time-stepping algorithm, we consider the three different scenes: (a) $\tau_{\max} = 0.1$, (b) $\tau_{\max} = 0.2$ and (c) $\tau_{\max} = 0.5$.

At first, we run a special R-IERK(2,4; c_2) method (taking $c_2 = 1$ for example) for the three different scenes. As expected, see Figure 3, the discrete energy curves are decreasing, and the energy curve is closer to the reference energy when a smaller τ_{\max} is adopted. The CPU time and the total number of time-level listed in Table 2 show the effectiveness and efficiency of the R-IERK(2,4;1) method (3.2) with $T = 450$. Surprisingly, the R-IERK(2,4;1) method performs well and generates reliable energy curves although it can not be covered by our theory, see Remark 1.

Table 2: CPU time and total time-level of R-IERK(2,4;1) method.

Time-stepping strategy	$\tau = 10^{-4}$	$\tau_{\max} = 0.1$	$\tau_{\max} = 0.2$	$\tau_{\max} = 0.5$
CPU time (in seconds)	6724.63	11.90	6.42	2.62
Time levels	4.5×10^6	11714	5840	2304

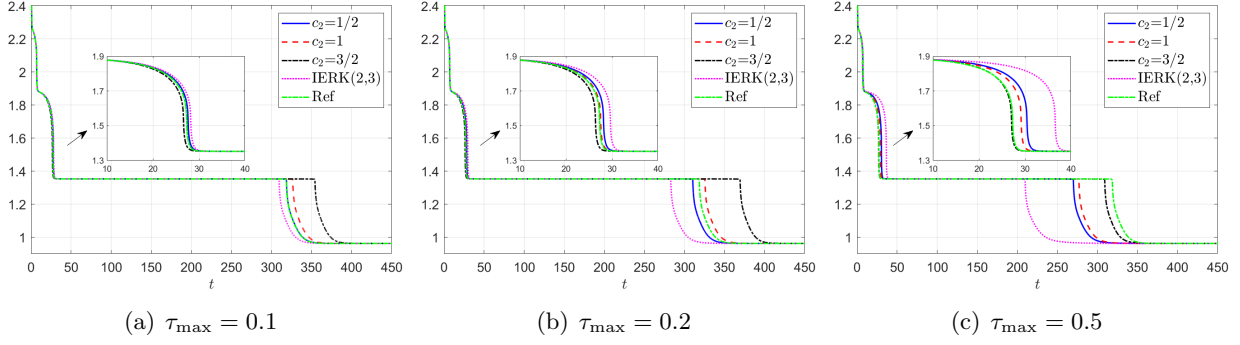


Figure 4: Energy behaviors of R-IERK(2,4; c_2) method (3.2) and IERK(2,3) method.

Figure 4 depicts the energy curves generated by the IERK(2,3) method and the R-IERK(2,4; c_2) method (3.2) with different parameters $c_2 = \frac{1}{2}, 1$ and $\frac{3}{2}$ for three different maximum time-steps: (a) $\tau_{\max} = 0.1$, (b) $\tau_{\max} = 0.2$ and (c) $\tau_{\max} = 0.5$. As expected, the discrete energy curves are all decreasing. It is seen that the energy curves of the IERK(2,3) method have significant changes for different maximum time-steps, while the discrete energy curves computed by the R-IERK(2,4; c_2) method (3.2) are relatively robust with respect to the change of time-steps. They suggest that the R-IERK(2,4; c_2) methods (3.2) with the $\tau_n \lambda_{\text{ML}}$ -independent average dissipation rates allow some larger adaptive step-sizes and would be more preferable in adaptive time-stepping simulations.

5.2 Tests of R-IERK(3,6; \hat{a}_{52}) methods

We examine the energy behaviors of the R-IERK(3,6; \hat{a}_{52}) method (3.4) with three different parameters $\hat{a}_{52} = \frac{2}{3}, \frac{7}{10}$ and $\frac{3}{4}$ for Example 1 with the adaptivity parameter $\eta = 500$. The reference solution is generated with $\tau = 10^{-4}$ by the Lobatto-type IERK3-2 method in [26] with the parameter $a_{43} = -\frac{3}{5}$, called IERK(3,5) method hereafter, which is regarded as the best one among the third-order IERK methods in [26] with the associated average dissipation rate $\mathcal{R}_L^{(3,5)} = \frac{5}{4} + \frac{2}{5}\tau\bar{\lambda}_{\text{ML}}$.

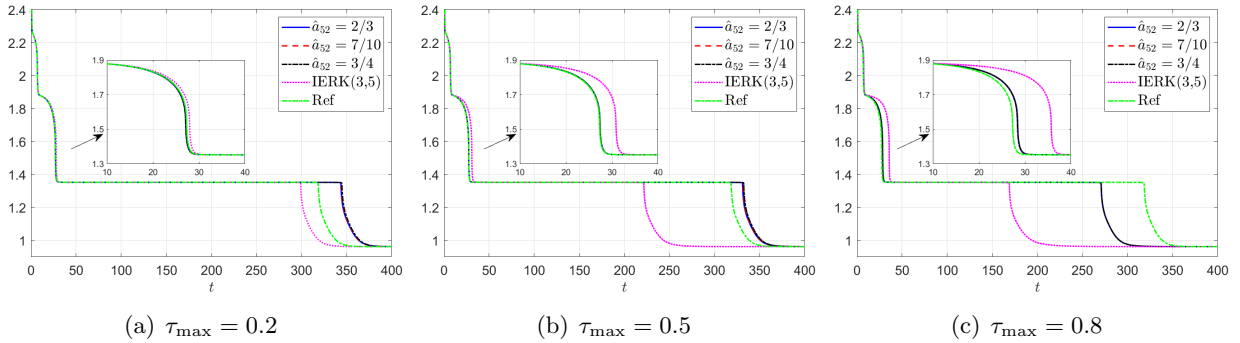


Figure 5: Energy behaviors of R-IERK(3,6; \hat{a}_{52}) method (3.4) and IERK(3,5) method.

Figure 5 depicts the energy curves of the IERK(3,5) method and the R-IERK(3,6; \hat{a}_{52}) method (3.4) for three different scenes: (a) $\tau_{\max} = 0.2$, (b) $\tau_{\max} = 0.5$ and (c) $\tau_{\max} = 0.8$. As seen, the energy curves generated by the R-IERK(3,6; \hat{a}_{52}) method are indistinguishable for all scenes, which seems to be accordant with the convergence tests in Figure 2 (b). More importantly, one can observe that the energy curves of the IERK(3,5) method have significant changes for different maximum time-steps, while the discrete energy curves computed by the R-IERK(3,6; \hat{a}_{52}) methods are relatively robust with

respect to the change of time-steps. They suggest that the R-IERK(3,6; \hat{a}_{52}) methods allow some larger adaptive step-sizes and would be more preferable in adaptive simulations.

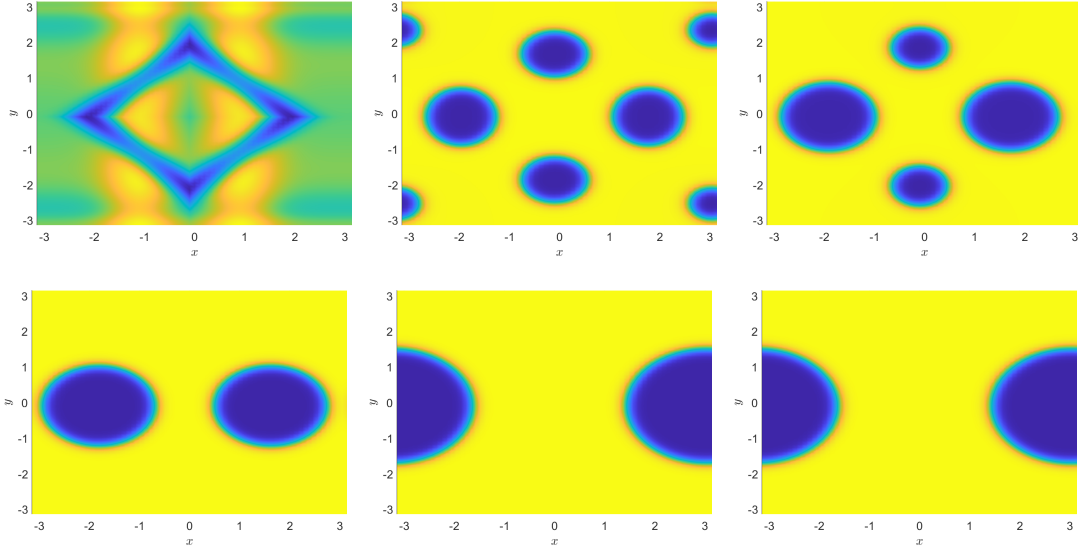


Figure 6: Solution profiles at $t = 0, 2, 20, 200, 450$ and 1000 generated by the R-IERK(3,6; $\frac{3}{4}$) method using the adaptive time-stepping with $\eta = 500$ and $\tau_{\max} = 0.5$.

The evolution of microstructure for the CH model due to the phase separation at different time are summarized in Figure 6, where the phase profiles at $t = 0, 2, 20, 200, 450$ and 1000 generated by the R-IERK(3,6; $\frac{3}{4}$) method using the adaptive time-stepping with $\eta = 500$ and $\tau_{\max} = 0.5$ are depicted. As seen, the microstructure is relatively fine and consists of many precipitations at early time and the coarsening, dissolution, merging processes are observed in approaching the steady state.

6 Concluding remarks

We propose a class of R-IERK methods in which the associated differentiation matrices and the average dissipation rates are always independent of the time-space discretization meshes. Numerical tests suggest that the R-IERK methods have significant robustness in self-adaptive time-stepping procedures as some larger adaptive step-sizes in actual simulations become possible. With the help of an updated time-space error splitting approach with discrete orthogonal convolution kernels and the Grönwall-type lemma for multi-stage methods, the uniform boundedness of stage solutions is theoretically verified without the global Lipschitz continuity assumption of nonlinear bulk so that one can establish the original energy dissipation laws at discrete time stages. Our analysis paves a new way to the internal nonlinear stability of some efficient (not necessarily algebraically stable) Runge-Kutta methods for semilinear parabolic problems. Actually it is closely related to the so-called internal stability analysis [12, 13], which will be useful to control the stability associated with each stage in addition to each step beyond traditional step-wise stability.

References

- [1] G. Akrivis, B. Li and D. Li, Energy-decaying extrapolated RK-SAV methods for the Allen-Cahn and Cahn-Hilliard equations, *SIAM J Sci. Comput.*, 41(6) (2019), pp. A3703-A3727.

- [2] U. Ascher, S. Ruuth and R. J. Spiteri, Implicit-explicit Runge-Kutta methods for time dependent partial differential equations, *Appl. Numer. Math.*, 25 (1997), pp. 151-167.
- [3] A. Cardone, Z. Jackiewicz, A. Sandu and H. Zhang, Extrapolated implicit-explicit Runge-Kutta methods, *Math. Model. Anal.*, 19:1 (2014), pp. 18-43.
- [4] W. Chen, X. Wang, Y. Yan and Z. Zhang, A second order BDF numerical scheme with variable steps for the Cahn-Hilliard equation, *SIAM J. Numer. Anal.*, 57(1) (2019), pp. 495-525.
- [5] M. Chen, F. Yu, Q. Zhang and Z. Zhang, Variable step-size BDF3 method for Allen-Cahn equation, *J. Comput. Math.*, 42(5) (2024), doi: 10.4208/jcm.2304-m2022-0140.
- [6] K. Cheng, C. Wang, S. Wise and X. Yue, A second-order, weakly energy-stable pseudo-spectral scheme for the Cahn-Hilliard equation and its solution by the homogeneous linear iteration method, *J. Sci. Comput.*, 69 (2016), pp. 1083-1114.
- [7] Q. Du, L. Ju, X. Li and Z. Qiao, Maximum bound principles for a class of semilinear parabolic equations and exponential time-differencing schemes, *SIAM Rev.*, 63 (2021), pp. 317-359.
- [8] Z. Fu, T. Tang and J. Yang, Energy diminishing implicit-explicit Runge-Kutta methods for gradient flows, *Math. Comput.*, 93 (2024), pp. 2745-2767.
- [9] Y. He, Y. Liu and T. Tang, On large time-stepping methods for the Cahn-Hilliard equation, *Appl. Numer. Math.*, 57 (2007), pp. 616-628.
- [10] J. Huang, C. Yang and Y. Wei, Parallel energy-stable solver for a coupled Allen-Cahn and Cahn-Hilliard system, *SIAM J. Sci. Comput.*, 42(5) (2020), pp. C294-C312.
- [11] G. Izzo and Z. Jackiewicz, Highly stable implicit-explicit Runge-Kutta methods, *Appl. Numer. Math.*, 113 (2017), pp. 71-92.
- [12] C. A. Kennedy and M. H. Carpenter, Additive Runge-Kutta schemes for convection-diffusion-reaction equations, *Appl. Numer. Math.*, 44 (2003), pp. 139-181.
- [13] C. A. Kennedy and M. H. Carpenter, Diagonally implicit Runge-Kutta methods for ordinary differential equations: a review, Technical Memorandum: NASA/TM 2016-219173, 2016.
- [14] D. Li and Z. Qiao, On second order semi-implicit Fourier spectral methods for 2D Cahn-Hilliard equations, *J. Sci. Comput.*, 70 (2017), pp. 301-341.
- [15] D. Li and Z. Qiao, On the stabilization size of semi-implicit Fourier-spectral methods for 3D Cahn-Hilliard equations, *Commun. Math. Sci.*, 15 (2017), pp. 1489-1506.
- [16] D. Li, Z. Qiao and T. Tang, Characterizing the stabilization size for semi-implicit Fourier spectral method to phase field equations, *SIAM J. Numer. Anal.*, 54 (2016), pp. 1653-1681.
- [17] D. Li, C. Quan and T. Tang, Stability and convergence analysis for the implicit-explicit method to the Cahn-Hilliard equation, *Math. Comput.*, 91(334) (2022), pp. 785-809.
- [18] B. Li, H. Gao and W. Sun, Unconditional optimal error estimates of a Crank-Nicolson Galerkin method for the nonlinear thermistor equations, *SIAM J. Numer. Anal.*, 52 (2014), pp. 933-954.

- [19] B. Li and W. Sun, Unconditional convergence and optimal error estimates of a Galerkin-mixed FEM for incompressible miscible flow in porous media, *SIAM J. Numer. Anal.*, 51 (2013), pp. 1959-1977.
- [20] J. Li, Z.-Z. Sun and X. Zhao, A three level linearized compact difference scheme for the Cahn-Hilliard equation, *Sci. China Math.*, 55(4) (2012), pp. 805-826.
- [21] H.-L. Liao and Z.-Z. Sun, Maximum norm error bounds of ADI and compact ADI methods for solving parabolic equations, *Numer. Methods Partial Differential Equ.*, 26(1) (2010), pp. 37-60.
- [22] H.-L. Liao, B. Ji and L. Zhang, An adaptive BDF2 implicit time-stepping method for the phase field crystal model, *IMA J. Numer. Anal.*, 42(1) (2022), pp. 649-679.
- [23] H.-L. Liao, B. Ji, L. Wang and Z. Zhang, Mesh-robustness of an energy stable BDF2 scheme with variable steps for the Cahn-Hilliard model, *J. Sci. Comput.*, 2022, 92: 52, doi: 10.1007/s10915-022-01861-4.
- [24] H.-L. Liao and X. Wang, Average energy dissipation rates of explicit exponential Runge-Kutta methods for gradient flow problems, *Math. Comput.*, 2024, doi: 10.1090/mcom/4015.
- [25] H.-L. Liao, X. Wang and C. Wen, Original energy dissipation preserving corrections of integrating factor Runge-Kutta methods for gradient flow problems, *J. Comput. Phys.*, 2024, 519: 113456.
- [26] H.-L. Liao, X. Wang and C. Wen, Average energy dissipation rates of additive implicit-explicit Runge-Kutta methods for gradient flow problems, arXiv:2410.06463v1, 2024, submitted.
- [27] H.-L. Liao and Z. Zhang, Analysis of adaptive BDF2 scheme for diffusion equations, *Math. Comput.*, 90 (2021), pp. 1207-1226.
- [28] X. Li, Z. Qiao and C. Wang, Convergence analysis for a stabilized linear semi-implicit numerical scheme for the nonlocal Cahn-Hilliard equation, *Math. Comput.*, 90 (2021), pp. 171-188.
- [29] J. Shen, T. Tang and L. Wang, Spectral methods: Algorithms, analysis and applications, Springer-Verlag, Berlin Heidelberg, 2011.
- [30] J. Shen, J. Xu and J. Yang, The scalar auxiliary variable (SAV) approach for gradient flows, *J. Comput. Phys.*, 353 (2018), pp. 407-416.
- [31] J. SHIN, H.-G. LEE AND J.-Y. LEE, Convex splitting Runge-Kutta methods for phase-field models, *Comput. Math. Appl.*, 73:11 (2017), pp. 2388-2403.
- [32] J. Shin, H.-G. Lee and J.-Y. Lee, Unconditionally stable methods for gradient flow using convex splitting Runge-Kutta scheme, *J. Comput. Phys.*, 347 (2017), pp. 367-381.
- [33] M. N. Spijker, Feasibility and contractivity in implicit Runge-Kutta methods, *J. Comp. Appl. Math.*, 12/13 (1985), pp. 563-578.
- [34] Z. Z. Sun, A second-order accurate linearized difference scheme for the two-dimensional Cahn-Hilliard equation, *Math. Comput.*, 64 (212) (1995), pp. 1463-1471.
- [35] L. Wang and H. Yu, On efficient second order stabilized semi-implicit schemes for the Cahn-Hilliard phase-field equation, *J. Sci. Comput.*, 77 (2018), pp. 1185-1209.
- [36] Z. Zhang and Z. Qiao, An adaptive time-stepping strategy for the Cahn-Hilliard equation, *Comm. Comput. Phys.*, 11(4) (2012), pp. 1261-1278.